INTRODUCTORY REVIEW

The 'wet mind': water and functional neuroimaging

Denis Le Bihan[1,2]

[1] NeuroSpin, Bâtiment 145, CEA Saclay, 91191 Gif-sur-Yvette, France
[2] Human Brain Research Center, Kyoto University Graduate School of Medicine, Kyoto, Japan

E-mail: denis.lebihan@cea.fr

Abstract
Functional neuroimaging has emerged as an important approach to study the brain and the mind. Surprisingly, although they are based on radically different physical approaches both positron emission tomography (PET) and magnetic resonance imaging (MRI) make brain activation imaging possible through measurements involving water molecules. So far, PET and MRI functional imaging have relied on the principle that neuronal activation and blood flow are coupled through metabolism. However, a new paradigm has emerged to look at brain activity through the observation with MRI of the molecular diffusion of water. In contrast with the former approaches diffusion MRI has the potential to reveal changes in the intrinsic water physical properties during brain activation, which could be more intimately linked to the neuronal activation mechanisms and lead to an improved spatial and temporal resolution. However, this link has yet to be fully confirmed and understood. To shed light on the possible relationship between water and brain activation, this introductory paper reviews the most recent data on the physical properties of water and on the status of water in biological tissues, and evaluates their relevance to brain diffusion MRI. The biophysical mechanisms of brain activation are then reassessed to reveal their intimacy with the physical properties of water, which may come to be regarded as the 'molecule of the mind'.

Introduction

Over the last 30 years functional neuroimaging has emerged as an important approach to study the brain and the mind. This has been possible because of significant advances mainly in two imaging modalities, namely positron emission tomography (PET) and magnetic resonance imaging (MRI). Although those two modalities are based on radically different physical approaches (detection of β^+ radioactivity for the first one and nuclear magnetization for the latest), both make brain activation imaging possible through measurements involving water molecules. This should come as no surprise, given that water constitutes nearly 80% of the
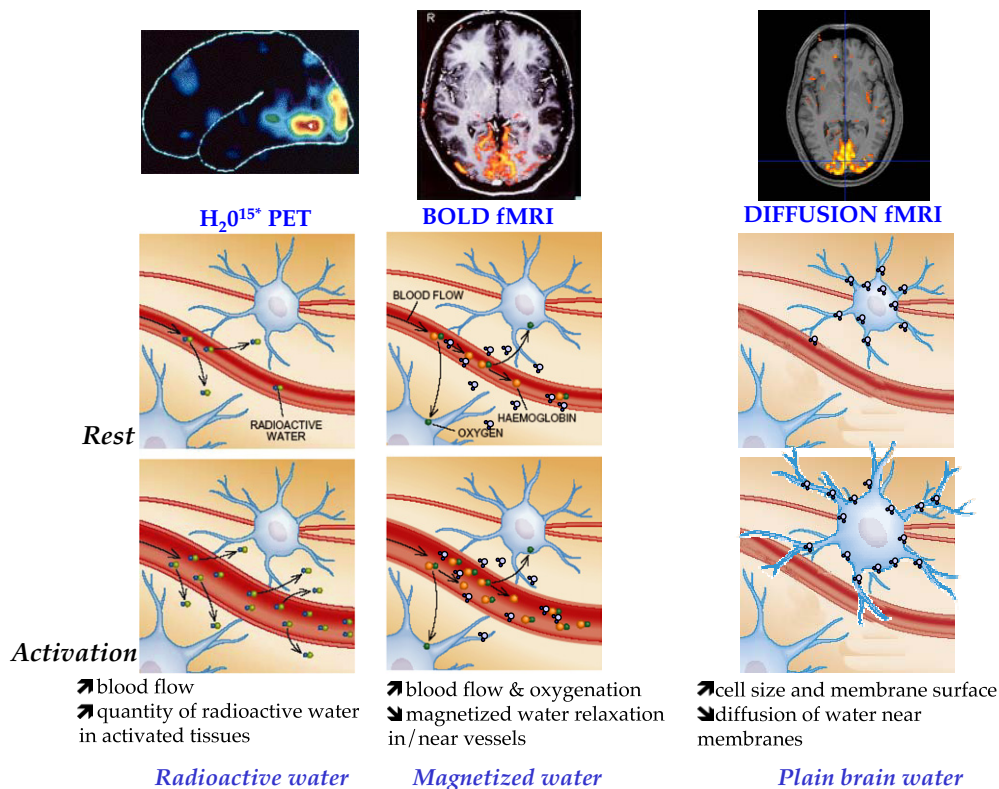
Figure 1. General principles of PET and MRI functional neuroimaging methods. Left: brain activation mapping with PET. Radioactive water (H_2O^{15}) is used as a tracer to detect neuronal activation-induced increases in blood flow. Middle: brain activation mapping with BOLD fMRI. Water magnetization in and around small vessels is modulated by the flow of red blood cells containing paramagnetic deoxyhaemoglobin. Adapted from Raichle (1994). Right: brain activation mapping with diffusion fMRI. The reduction in water diffusion which occurs during activation is thought to originate from a membrane-bound water layer which expands during activation-induced cell swelling. While with PET and BOLD fMRI water is only an indirect means to detect changes in blood flow through the imaging scanner, the changes in water properties seen with diffusion fMRI seem to be an intrinsic part of the activation process.

brain weight and 90% of its molecules. So far, PET and MRI functional imaging have relied on the same principle that neuronal activation and blood flow are coupled through metabolism (Roy and Sherrington 1890): blood flow increases locally in activated brain regions. In the case of PET one uses H_2O^{15} radioactive water which is produced by using a cyclotron and injected into the subject's vasculature. In activated brain regions, the increase in blood flow leads to a local increase in the tissue radioactive water content detected and localized by the PET camera (Posner *et al* 1988, Fox *et al* 1986, Raichle 1994). With MRI the hydrogen nuclei of brain endogenous water molecules are magnetized by a strong external magnetic field. In activated regions the increase in blood flow results in an increase of blood oxygenation which slightly modifies, in and around blood vessels, the magnetization relaxation properties of the water molecules detected by the MRI scanner (so-called BOLD—blood oxygen level dependent—effect (Ogawa *et al* 1993, Kwong *et al* 1992)). In both approaches water is, thus, merely an indirect means to observe the changes in cerebral blood flow which accompany brain activation (figure 1).

Although PET and BOLD fMRI have been extremely successful for the functional neuroimaging community (Raichle and Mintun 2006), they present well-known limitations. While the coupling between neuronal activation, metabolism and blood flow has been verified in most instances for BOLD fMRI (Logothetis *et al* 2001, Logothetis and Wandell 2004), the degree and the mechanism of this coupling is not fully understood (Mangia *et al* 2003, Magistretti and Pellerin 1999) and may even fail under some pathological conditions (Lehericy *et al* 2002) or in the presence of drugs. Also, it has been pointed out that the spatial functional resolution of vascular-based functional neuroimaging might be limited, because vessels responsible for the increase of blood flow and blood volume feed or drain somewhat large territories which include clusters of neurons with potentially different functions (Turner 2002). Similarly the physiological delay necessary for the mechanisms triggering the vascular response to work intrinsically limits the temporal resolution of BOLD fMRI, although some vascular-related signals, such as the cerebral blood volume (Lu *et al* 2005) or the total local haemoglobin concentration measured by diffuse optical imaging (Huppert *et al* 2006) could precede typical BOLD time courses.

On the other hand, a fundamentally new paradigm has emerged to look at brain activity through the observation with MRI of the *diffusion* behaviour of the water molecules (Darquie *et al* 2001). It has been shown that the diffusion of water slightly slows down in the activated brain cortical areas. This slowdown, which occurs several seconds before the haemodynamic response detected by BOLD fMRI (Le Bihan *et al* 2006), has been described in terms of a phase transition of the water molecules from a somewhat fast to a slower diffusion pool in the cortex undergoing activation and tentatively ascribed to the membrane expansion of cortical cells which undergo swelling during brain activation (figure 1). This hypothetical mechanism, which remains to be confirmed, would mark a significant departure from the former blood-flow-based PET and MRI approaches, and would potentially offer improved spatial and temporal resolution, due to its more intimate link to neuronal activation. However, the step might even extend further: in contrast with the former approaches based on changes in *artificially* induced water physical properties, namely radioactivity and magnetization, required for the external PET or MRI detection, the new, diffusion-based approach, merely uses MRI as a means to reveal changes in *intrinsic* water physical properties. These changes in the diffusion behaviour of water during activation might be indeed an *active* component of this process, as water homeostasis and water movement have without any doubt a central role in brain physiology.

There is an abundant and recent literature on the physical properties of water in biological tissues in one hand, and on the cellular events underlying brain activation on the other hand. However, this literature may not be so familiar to the neuroimaging community. The aim of this paper is, therefore, to review the most recent data on the physical properties of water and on the status of water in biological tissues, and to evaluate their relevance to brain diffusion MRI. The literature on the brain activation biophysical mechanisms is then assessed to shed light on their intimacy with the physical properties of water. Although this review provides a framework for diffusion MRl imaging, it should be considered more as a kind of brainstorming introduction to the field.

Water diffusion MRI: outstanding issues

Principles of diffusion MRI

Non-invasive imaging methods usable in living animals and humans currently have a macroscopic (millimetre) resolution. Hence, access to dynamic tissue microstructure must be

provided through physical processes encompassing several spatial scales. Molecular diffusion is an exquisite example of such a multiscale integrated process by which fluctuations in molecular random motion at microscopic scale can be inferred from observations at a much larger scale using statistical physical models, although the individual molecular structure and pathway is completely ignored. This powerful multiscale approach allowed Einstein indirectly to demonstrate the existence of atoms through the identification of diffusion with Brownian motion in the framework of the molecular theory of heat (Einstein 1956). Over the last 20 years it has been shown that magnetic resonance imaging (MRI) could provide *macroscopic* and quantitative maps of water molecular diffusion (Le Bihan and Breton 1985, Taylor and Bushell 1985), especially in the brain (Le Bihan *et al* 1986), to make indirect inferences on the *microstructure* of biological tissues.

As the diffusion coefficient of water in brain tissue at body temperature is about 1×10^{-3} mm^2 s^{-1} the Einstein's diffusion equation ($\langle z^2 \rangle = 2DT_d$, where $\langle z^2 \rangle$ is the mean free quadratic displacement in one direction, D is the diffusion coefficient and T_d is the diffusion time) (Einstein 1956) indicates that about two thirds of diffusion-driven molecular displacements are within a range not exceeding 10 μm during diffusion times currently used with MRI (around 50 ms), well beyond typical image resolution. Indeed, water molecules move in the brain while interacting with many tissue components, such as cell membranes, fibres or macromolecules, etc, and the indirect observation of these displacements embedded into the diffusion coefficient provides valuable information on the microscopic obstacles encountered by diffusing molecules, and in turn, on the structure and the geometric organization of cells in tissues, such as cell size or cell orientation in space (see Le Bihan (2003) for a review).

However, the overall signal observed in a 'diffusion' MRI image volume element (voxel), at a *millimetric* resolution, results from the integration, on a statistical basis, of all the *microscopic* displacement distributions of the water molecules present in this voxel, and some modelling is necessary to make inferences between those two scales. As a departure from earlier diffusion studies in biological studies when efforts were made to depict the physical elementary diffusion process (Tanner 1979, 1978, Cooper *et al* 1974), it was suggested for simplicity to portray the complex diffusion patterns which occur in a biological tissue within a voxel by using the free diffusion physical model (where the distribution of molecular displacements obeys a Gaussian law), but replacing the physical diffusion coefficient, D, with a global parameter, the *apparent diffusion coefficient* (ADC) (Le Bihan *et al* 1986). In practice the MRI signal is made sensitive to the diffusion-driven water molecular displacements through variations in space of the magnetic field, so-called magnetic field gradients. In the presence of those gradients, any molecular displacement occurring during a given time interval (diffusion time) produces a phase shift of the associated MRI signal. Due to the very large number of water molecules present in each image voxel, the phase shifts are distributed, reflecting the diffusion-driven displacement distribution, resulting in a loss of coherence, and, hence, an attenuation of the MRI signal. This attenuation, A, can then be simply formulated as

$$A = S/S_0 = \exp(-b\,\mathrm{ADC}) \tag{1}$$

where b is the degree of diffusion sensitization (as defined by the amplitude and the time course of the magnetic field gradient pulses used to encode molecular diffusion displacements (Le Bihan 1995)), S is the signal at a particular b-value, S_0 is the signal at $b = 0$. However, one should bear in mind that, strictly speaking, the MRI signal is actually sensitive to the diffusion path of the hydrogen nuclei carried by water molecules, not the diffusion coefficient per se.

The ADC concept has been widely adopted in the literature. Potential applications of water diffusion MRI, which were suggested very early in Le Bihan *et al* (1986), are many (Le Bihan 2003), but the most successful clinical application since the early 1990s has been
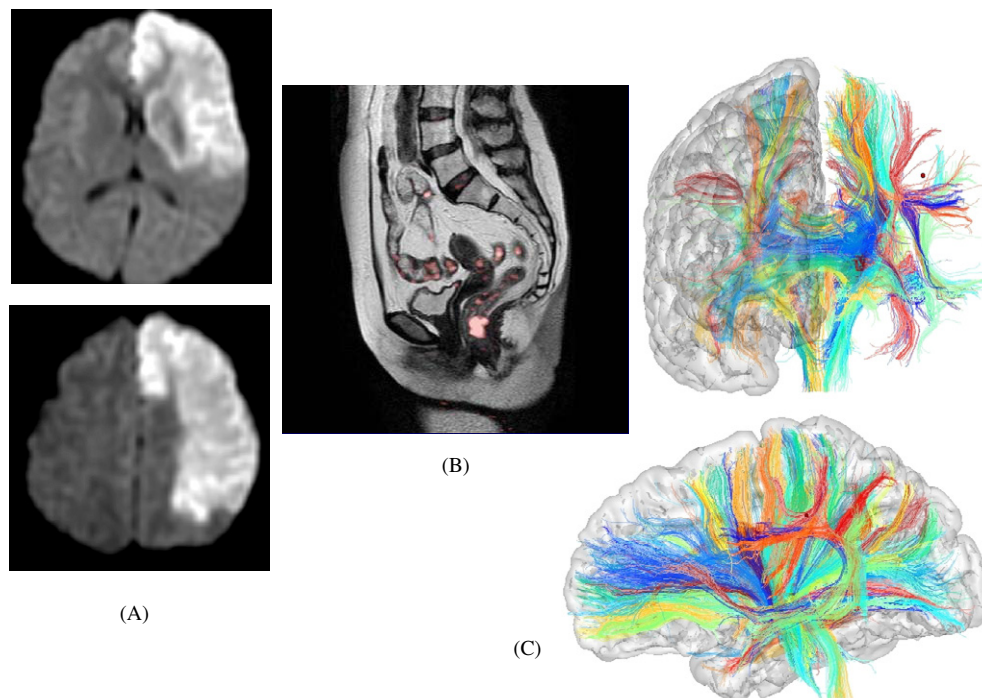
Figure 2. Major current applications of diffusion MRI. (A) Diffusion MRI in brain acute stroke. The region with bright signal correspond to brain regions where water diffusion is reduced, as a result of acute cerebral ischaemia and associated cytotoxic oedema. Image courtesy of Dr Openheim (Radiology Department, Hôpital Saint-Anne, France). (B) Diffusion MRI in cancer. Coloured areas correspond to regions where the water diffusion coefficient is decreased. Such regions have been shown to match areas where malignant cells are present (primary lesion or metastases). Image courtesy of Dr Koyama (Radiology Department, Kyoto University, Graduate School of Medicine, Kyoto, Japan). (C) Diffusion and brain white matter fibre tracking. Water diffusion in brain white matter is anisotropic. As a result it is possible to determine for each voxel of the image the direction in space of the fibres. Using post-processing algorithms the voxels can be connected to produce colour-coded images of the putative underlying white matter tracts. Images courtesy of Y Cointepas, M Perrin and C Poupon (SHFJ/CEA, Orsay, France).

acute brain ischaemia, as the ADC sharply drops in the infarcted regions, minutes after the onset of the ischaemic event (Moseley *et al* 1990b) (figure 2). With its unmatched sensitivity diffusion MRI provides some patients with the opportunity to receive suitable treatment at a stage when brain tissue might still be salvageable (Warach and Baron 2004). However, the exact mechanism responsible for this ADC drop remains poorly understood, although cell swelling through cytotoxic oedema seems to play a major part (Sotak 2002). Another potentially important clinical application is the detection of cancer and metastases. The water ADC is significantly decreased in malignant tissues, and body diffusion MRI (Takahara *et al* 2004) is currently under evaluation as a potential alternative approach to fluoro-deoxyglucose (FDG)-PET (Ide 2006, Siegel and Dehdashti 2005) to detect malignant lesions (figure 2). Here also the origin of this diffusion anomaly is not clear, but somewhat linked to the cell proliferation.

On the other hand, as diffusion is a three-dimensional process, molecular mobility in tissues may not be the same in all directions. Diffusion anisotropy was observed at the end of the 1980s in brain white matter (Moseley *et al* 1990a). Diffusion anisotropy in white matter

originates from its specific organization in bundles of more or less myelinated axonal fibres running in parallel: diffusion in the direction of the fibres is faster than in the perpendicular direction, although the exact contribution of the white matter elements involved (intra- and extra-axonal compartments, membranes, myelin, etc) is still elusive. It appeared quickly, nevertheless, that this feature could be exploited to map out the orientation in space of the white matter tracks in the brain (Douek *et al* 1991). With the introduction of the more rigorous formalism of the *diffusion tensor* (Basser *et al* 1994), diffusion anisotropy effects could be fully extracted, characterized and exploited, providing even more exquisite images of white matter tracks (figure 2) and brain connectivity (see Le Bihan *et al* (2001), Le Bihan (2003) for reviews).

However, the most recent development of diffusion MRI is its application to the field of brain *functional* imaging (Darquie *et al* 2001, Le Bihan *et al* 2006). Diffusion MRI has been thought to visualize dynamic tissue changes associated with neuronal activation, a much more direct approach than BOLD fMRI (figure 1). Clearly, the mechanisms underlying the small observed water diffusion dropout have entirely to be clarified. However, there is already a large body of knowledge out in the literature suggesting that those diffusion changes might well result from the peculiar properties of water in biological tissues, and on their association with the biophysical events underlying neuronal activation. This literature is reviewed in the next sections, but it should be understood that this review does not directly represent a 'proof' for the suggested diffusion MRI mechanisms which remain to be validated by future experimental work.

Water diffusion in biological tissues

The ADC in the brain is two to ten times smaller than free water diffusion in an aqueous solution (which is 2.272 mm^2 s^{-1} at 25 °C), as measured by nuclear magnetic resonance (Bratton *et al* 1965, Cope 1969, Hazlewood *et al* 1991, Kasturi *et al* 1980) or neutron scattering methods (Trantham *et al* 1984). High viscosity, macromolecular crowding and restriction effects have been proposed to explain the water diffusion reduction in the intracellular space (Hazlewood *et al* 1991), and tortuosity effects for water diffusion in the extracellular space (Nicholson and Philipps 1981, Chen and Nicholson 2000). Restricted diffusion effects, for instance, may be evaluated by changing the diffusion time (Cooper *et al* 1974, Latour *et al* 1994b): the displacements of the molecules become limited when they reach the boundaries of close spaces and the diffusion coefficient artificially goes down with longer diffusion times. Variations of the ADC with the diffusion times have been reported in the brain (Norris *et al* 1994, Assaf and Cohen 1998). However, no clear restriction behaviour has been observed *in vivo* for water in the brain, as the diffusion distance seems to increase well beyond cell dimensions with long diffusion times (Le Bihan *et al* 1993, Moonen *et al* 1991), or even in cell suspensions (Garcia-Perez *et al* 1999). Furthermore, studies have established long ago that the overall low diffusivity of water in cells could not be fully explained by compartmentation (restriction) effects from cell membranes nor by scattering or obstruction (tortuosity) effects from cellular macromolecules (Rorschach *et al* 1973, Chang *et al* 1973, Colsenet *et al* 2005). This strongly suggests that the cellular components responsible for the reduced diffusion coefficient in biological tissues are much smaller than the diffusion length currently used with MRI. In summary, the cell membranes in the brain, although they likely hinder the water diffusion process ('hindered' diffusion, as opposed to strictly 'restricted' diffusion), seem highly permeable to water, either passively or through transporters, such as the specific aquaporin channels which have been found abundant in the brain (Amiry-Moghaddam and Ottersen 2003).
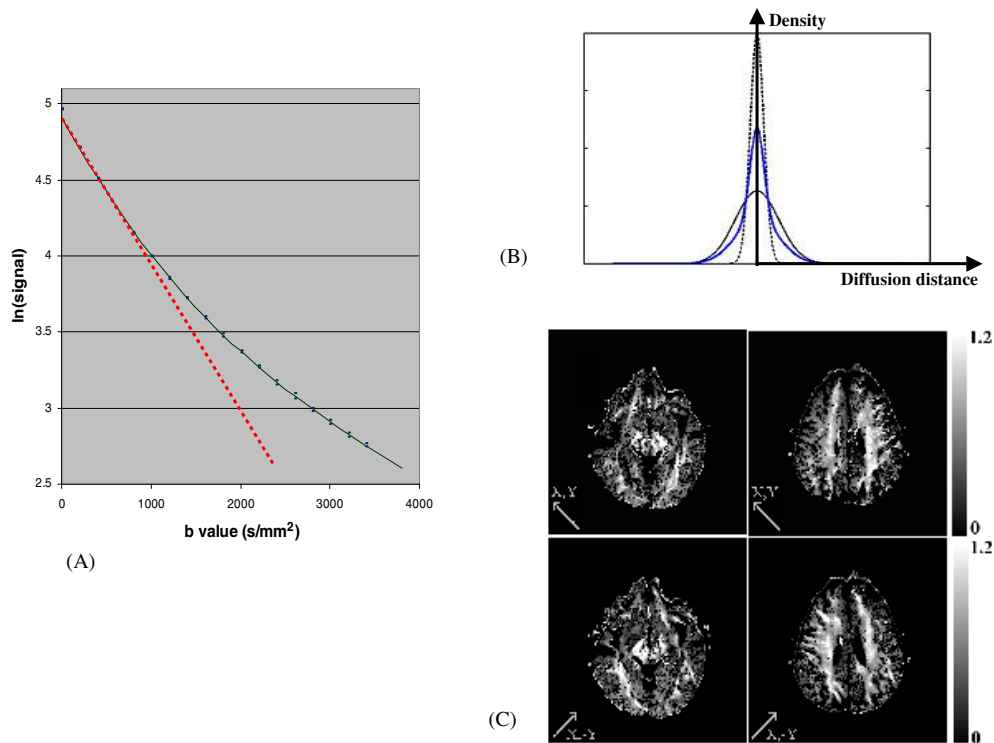
Figure 3. Water diffusion in the brain is not a free random walk process. (A) Plot of the signal attenuation as a function of the degree of diffusion-sensitization (*b*-value) in the human visual cortex. The plot is clearly not linear and best described using a biexponential model. (B) Plot of a q-space analysis which gives the distribution of the diffusion-driven displacement of the water molecules. The distribution is not Gaussian, but well approximated by the sum of two Gaussian distributions, suggesting the presence of two water phases with slow or intermediate exchange. (C) Kurtosis maps. The deviation from a Gaussian distribution can be evaluated by calculating an index of kurtosis based on the second moment of the displacement distribution. The images show the value of this index within two brain slices and two orientations of the diffusion-sensitizing measurements (an index of zero indicates a Gaussian distribution). Water diffusion in the brain is clearly not Gaussian, especially in white matter. Courtesy of S Chabert (SHFJ/CEA, Orsay, France).

Indeed, many studies have experimentally established that the water diffusion-sensitized MRI signal attenuation in brain tissue (and other tissues as well) as a function of the sensitization (*b*-value) could not be well described by a single exponential decay, as would have been expected (equation (1)) in an unrestricted, homogenous medium (free Brownian diffusion) (Le Bihan 2003). Furthermore, diffusion data gathered using the 'q-space' approach, a technique which provides estimates of the distribution of the diffusion-driven molecular displacements, clearly demonstrate that the water diffusion process cannot be modelled by a single Gaussian distribution (Cohen and Assaf 2002) (figure 3).

In most cases data have been very well fitted, however, with a biexponential function corresponding to two water diffusion pools or phases in *slow* exchange, with a fast and a slow diffusion coefficient (Niendorf *et al* 1996, Assaf and Cohen 1998):

$$S = S_0 f_{\text{slow}} \exp(-b\, D_{\text{slow}}) + S_0 f_{\text{fast}} \exp(-b\, D_{\text{fast}}) \tag{2}$$

Table 1. Water diffusion parameters in the human visual cortex.

f_{fast}	0.67 ± 0.02
f_{slow}	0.33 ± 0.02
D_{fast}	$1.27 \pm 0.19 \text{ mm}^2 \text{ s}^{-1}$
D_{slow}	$0.27 \pm 0.05 \text{ mm}^2 \text{ s}^{-1}$

These parameters were estimated by fitting the MRI signal in a region of interest placed in the visual cortex of seven subjects acquired using 16 different b-values (0 to 3400 s mm^{-2}) with equation (2).

where f and D are the volume fraction and the diffusion coefficient associated with the slow and fast diffusion phases (SDP and FDP, respectively), with $f_{\text{slow}} + f_{\text{fast}} = 1$ (in this simple model differences in T_2 relaxation are not taken into account). This biexponential model remains valid when the exchange regime becomes 'intermediate', but one has to replace the values for $f_{\text{slow,fast}}$ and $D_{\text{slow,fast}}$ in equation (2) by more complex parameters also taking into account the residence time of the molecules in the fast and slow compartments relative to the measurement time in a more realistic manner (Karger *et al* 1988).

Studies performed by Niendorf *et al* (1996) in the rat brain *in vivo* (with b factors up to 10 000 s mm^{-2}) using this model yielded $\text{ADC}_{\text{fast}} = (8.24 \pm 0.30) \times 10^{-4} \text{ mm}^2 \text{ s}^{-1}$ and $\text{ADC}_{\text{slow}} = (1.68 \pm 0.10) \times 10^{-4} \text{ mm}^2 \text{ s}^{-1}$ with $f_{\text{fast}} = 0.80 \pm 0.02$ and $f_{\text{slow}} = 0.17 \pm 0.02$. Similar measurements have been made in the human brain using b factors up to 6000 s mm^{-2}. The estimates for those diffusion coefficients and the respective volume fractions of those pools (table 1) have been strikingly consistent across the literature (Mulkern *et al* 1999, Maier *et al* 2001, Clark and Le Bihan 2000, Le Bihan *et al* 2006), providing at least some phenomenological validation of the biexponential model.

It has been often considered that the extracellular compartment might correspond to the FDP, as water would be expected to diffuse more rapidly there than in the intracellular, more viscous compartment. However, the volume fractions of the two water phases obtained using the biexponential model do not agree with those known for the intra- and extracellular water fractions ($F_{\text{intra}} \geqslant 0.80$ and $F_{\text{extra}} \leqslant 0.20$ (Nicholson and Sykova 1998)), even by taking into account differences in T_2 relaxation contributions between those compartments, so that the nature of those phases has yet remained unclear (LeBihan and van Zijl 2002). Furthermore, some careful studies have shown that such a biexponential diffusion behaviour could also be seen solely within the intracellular compartment, pointing out that both the SDP and FDP probably coexist within the intracellular compartment. Such studies were sometimes conducted with ions or molecules much larger than water, such as N-acetyl-aspartate (Assaf and Cohen 1998), fluoro-deoxy-glucose, or in particular biological samples, such as giant oocytes (Sehy *et al* 2002a, 2002b), so that extrapolation to water diffusion in neuronal tissues requires some caution. Theoretical models have shown that restriction caused by cylindrical membranes can also give rise to a pseudo-biexponential diffusion behaviour in nerves (Stanisz *et al* 1997). Other models have been introduced, for instance based on a combination of extra-axonal water undergoing hindered diffusion and intra-axonal water undergoing restricted diffusion (Assaf *et al* 2004). Although such models could account for a pseudo-biexponential diffusion behaviour and diffusion anisotropy in white matter, it remains to be seen how it could be applied to the brain cortex, given that true restricted diffusion effects have not been really observed for water in the brain (see above).

In summary, there is growing indication that a direct relationship between the intracellular and extracellular volumes and the biexponential parameters of the diffusion attenuation could probably not be established, and several groups have underlined the important role of dynamic

parameters, such as membrane permeability and water exchange (Karger *et al* 1988, Chin *et al* 2004, Novikov *et al* 1998), and geometrical features, such as cell size distribution or axons/dendrite directional distribution (Chin *et al* 2004, Yablonskiy *et al* 2003, van der Weerd *et al* 2002, Kroenke *et al* 2004). Noticeably, however, those distinct models lead to a diffusion signal decay which is nevertheless well approximated by a biexponential fit (Chin *et al* 2004, Yablonskiy *et al* 2003, Sukstanskii *et al* 2004).

Variations of water diffusion with cell size

On the other hand, a second ensemble of experimental findings suggest that the *changes* of the volume fractions of the intra- and extracellular spaces which result from cell swelling and shrinking in different physiological, pathological or experimental conditions always lead to *variations* of the ADC. The drop of ADC which is observed during acute brain ischaemia has been clearly correlated with the cell swelling associated with cytotoxic oedema (Sotak 2004, Van Der Toorn *et al* 1996). Variations in the tortuosity coefficient, λ, within the extracellular space, linked to the increased diffusion path lengths caused by obstructing cells, have been considered as a potential source of diffusion reduction within the extracellular space (the diffusion reduction, D/D_0, where D_0 is the free diffusion coefficient, would scale as $\approx 1/\lambda^2$ (Thorne and Nicholson 2006)). It is not questionable that the tortuosity of the extracellular space modulates the diffusion process for some molecules or ions, such as TMA^+ (tetramethylammonium) which is much larger than water (and, hence, more sensitive to hindrance effects) and must be directly introduced into the extracellular space (Chen and Nicholson 2000, Nicholson and Sykova 1998). Extracellular space tortuosity for molecules, such as metabolites or neurotransmitters, has an important role in brain physiology and neural function. However, this importance of this mechanism is not so clear for *water*. Water diffusion studies (mainly conducted with MRI), whether *in vivo* or in tissue preparations, variations of the ECS tortuosity have always been induced by changes in the cellular volume. Hence, the observations of ADC changes are linked to both the changes in cellular volume *and* resulting extracellular space, and there is no way to untangle those two effects. So one cannot establish for water that the changed tortuosity is *at the origin* of the ADC change, but merely that *it is correlated with it*. The change in cellular volume might just as well be responsible per se (see below).

Further works have also established that the variations in *size* of the intra- and extracellular compartments correlate well with the observed changes in the *fraction* of the slow and fast diffusion pools of the biexponential model (Niendorf *et al* 1996, Benveniste *et al* 1992, OShea *et al* 2000, Hasegawa *et al* 1996, Dijkhuizen *et al* 1999, Van Der Toorn *et al* 1996). For instance, the ADC decrease which results from ouabain-induced cell swelling in perfused rat hippocampal slices has been shown to result in an increase of the SDP fraction, but the SDP and FDP diffusion coefficients *do not change* (Buckley *et al* 1999) (figure 4). These results suggest that the global water ADC decrease does not result from the increase in extracellular tortuosity induced by the shrinking of the extracellular space caused by cell swelling, but rather from a shift of balance between the fast and the slow diffusion water pools. An increase in tortuosity would lead to a decrease of the fast diffusion coefficient (assuming that the FDP corresponds to the extracellular space, which seems doubtful as explained above). The idea that obstruction by cells does not seem to be the principal source of diffusion reduction for water is also supported by the fact that the *highest* observable ratio, D/D_0, for water in the brain would be around $1.3/3 \approx 0.43$ ($D_0 \approx 3 \times 10^{-3}\,\mathrm{mm^2\,s^{-1}}$ at brain temperature), corresponding to $\lambda \leqslant 1.5$, in the range of the values found experimentally for small molecules by several groups (Nicholson and Tao 1993). This is smaller that the theoretical tortuosity index (1.63–1.72)
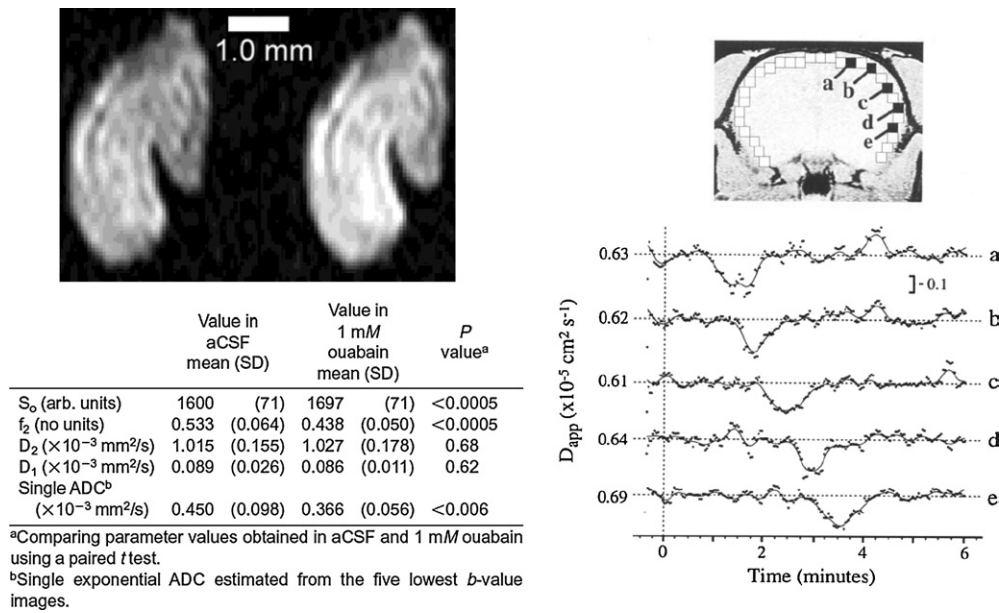
	Value in aCSF mean (SD)		Value in 1 mM ouabain mean (SD)		P value[a]
S_0 (arb. units)	1600	(71)	1697	(71)	<0.0005
f_2 (no units)	0.533	(0.064)	0.438	(0.050)	<0.0005
D_2 ($\times 10^{-3}$ mm²/s)	1.015	(0.155)	1.027	(0.178)	0.68
D_1 ($\times 10^{-3}$ mm²/s)	0.089	(0.026)	0.086	(0.011)	0.62
Single ADC[b] ($\times 10^{-3}$ mm²/s)	0.450	(0.098)	0.366	(0.056)	<0.006

[a]Comparing parameter values obtained in aCSF and 1 mM ouabain using a paired t test.
[b]Single exponential ADC estimated from the five lowest b-value images.

Figure 4. ADC decrease in extraphysiological brain challenges. (A) MRI diffusion-sensitised images ($b = 1980$ s mm^{-2}) of a rat brain hippocampus slice in artificial CSF (left) and in 1 mM ouabain solution (right). The signal is higher (decreased ADC) in the presence of ouabain which is known to induce cell swelling by inhibiting the Na$^+$/K$^+$ pumps. Analysis of the data using the biexponential (biphasic) model indicates that the water diffusion coefficients of the slow (D_1) and the fast (D_2) components do not change during the osmotic challenge. The decrease in ADC is solely the result of a decrease in the fast diffusing fraction (f_2) or, in other words, an increase of the slow diffusion fraction. Reprinted with permission from the publisher from Buckley *et al* (1999). (B) Time course of the diffusion coefficient in five regions ('a' through 'e' shown on the anaesthetized rat brain MRI image) separated by 7 mm in space during a spreading depression wave induced by a KCl application. The decrease in the diffusion coefficient is about 35% and lasts about 1 min. The decreased diffusion wave propagates along the cortex at a speed of 3.5 mm min^{-1}. Reprinted with permission from the publisher from Latour *et al* (1994a).

found by Thornes and Niholson (2006) for infinitely small molecules solely based on geometric considerations. Clearly, other mechanisms than obstruction by cell geometry should be considered.

Furthermore, earlier work on animal models has also shown that a decrease in water diffusivity could be visualized using MRI during intense neuronal activation, such as during status epilepticus induced by bicucculine (Zhong *et al* 1993) or cortical electroshocks (Zhong *et al* 1997) (figure 4). This diffusivity drop propagates along the cortex at a speed of about 1–3 mm min^{-1}, consistent with spreading depression (Busch *et al* 1996, Hasegawa *et al* 1995, Latour *et al* 1994a, Mancuso *et al* 1999, Röther *et al* 1996). Here also the diffusion drop (Hasegawa *et al* 1995, Latour *et al* 1994a, Mancuso *et al* 1999, Röther *et al* 1996) has been correlated to cell swelling (Dietzel *et al* 1980, Phillips and Nicholson 1979, Hansen and Olsen 1980).

More recently, the biexponential model has also been used to explain the diffusion changes observed in the activated brain visual cortex (Le Bihan *et al* 2006). As in the study by Buckley *et al* (1999) it has also been found that the SDP fraction was increasing, at the expense of the FDP, but that the SDP and FDP diffusion coefficients remained unchanged, which means

Table 2. Concentration of major ions in intra- and extracellular compartments (from http://www.lsbu.ac.uk/water/).

Ion	Ionic radius (Å)	Surface charge density	Molar ionic volume[a] (cm^3)	Intracellular (mM)	Extracellular (mM)
Ca^{2+}	1.00	2.11	−28.9	0.1	2.5
Na^+	1.02	1.00	−6.7	10	150
K^+	1.38	0.56	+3.5	159	4

[a] Molar aqueous ionic volume, cm^3 mol^{-1}, 298.15 K; negative values indicate contraction in volume (i.e. addition of the ions reduces the volume of the water).

that some water molecules undergo a change from a fast to a slow diffusing phase. At this point, it becomes obvious that the origin of the biphasic behaviour of water diffusion in brain tissue must be reconsidered, with a fresh look on the known status of water in cells and the experimental variations of the water diffusion coefficient with cell size. As this behaviour seems to be general to most tissue types, a valid model should accommodate both brain cortex and white matter, as well as body tissues, and account for physiological and pathological observations.

Water and membranes in biological tissues

Current cell-membrane model

In the 19th century, it was recognized that the cell contents form a 'gelatinous substance'. The concept of the membrane was introduced slightly later to account for the absence of mixing between the cytoplasm and the surrounding solution (the membrane, which is about 7.5–10 nm in thickness, could not be seen, of course, at that time). The membrane soon became 'semi-permeable', allowing water to pass, but not solutes. Later on, the discovery that some ions, notably K^+, could also pass through the membrane, led to the concept of 'membrane channels' which allow specific solutes to pass under some conditions (Boyle and Conway 1941). This simple model apparently explained how K^+ could accumulate within cells to partially compensate the negative charges of the proteins (so-called Donnan equilibrium), while Na^+ would remain largely excluded from the cytoplasm (table 2).

With this model, cell volume variations would result from changes in the osmotic balance between the intra- and extracellular compartments. Since then, the membrane has been physically observed and identified as a phospholipid bilayer with protein insertions, and a considerable number of types of channels have been identified and isolated, including water channels (aquaporins) (Agre 2005, Agre *et al* 2004) which have also been found in the brain (Amiry-Moghaddam and Ottersen 2003). Because so many solutes were found to pass through the membrane channels, the concept of 'pumps' was introduced (Glynn 2002). Those pumps take charge of cell housekeeping, maintaining the right concentration gradients between the cytoplasm and the surrounding medium, and a very large number of pumps have been proposed to accommodate many substances, ions, sugars, amino-acids, etc. In summary the cell membrane model has become extraordinarily complex, with the presence of a large quantity of channels and pumps at its surface, and water and ionic transmembrane shifts are required to maintain the ion homeostasis during neuronal activity.

Yet some authors have questioned this model, or more exactly its functional role (Ling *et al* 1967, Pollack 2001). The first of their arguments relates to the cell energy supply. It has been estimated that the Na^+ pump, in the current scheme, would consume by itself a third

to a half of the cell energy supply to maintain the extra/intracellular Na^+ gradient (Whittam 1961). As there are even many more other membrane channels and pumps (including those on the cell organelle surface, particularly high membrane density mitochondria), it is unclear how the cell produces the necessary amount of energy to maintain all of its concentration gradients solely from pumps (Ling 1988, Pollack 2003). Indeed, when the cell is deprived of energy, the normal intracellular concentrations of Na^+ and K^+ are maintained for hours (Ling 1997), suggesting that the basic solute partitioning is assumed by other, less energy demanding mechanisms. The channel-pump systems would be involved to carry more specialized tasks or transient perturbations, recoveries or modulations of the general balance, perhaps even in specific regions of the cell. Other groups have also demonstrated that the Na^+/K^+ and other gradients could be maintained for hours and the cell function normally even after the cell membrane was largely disrupted or even removed by different technical means (Kellermayer *et al* 1986), as long as the cell proteins remain in the cytoplasm (Cameron *et al* 1996, Fullerton *et al* 2006). Actually, diffusion of macromolecules in the crowded cytoplasm is extremely slow (Arrio-Dupont *et al* 2000, Luby-Phelps *et al* 1986, Seksek *et al* 1997) and macromolecules are expected to stay within the cytoplasm hours after the cell membrane has been removed.

In view of these observations it has been suggested that, whereas the membrane could be seen as essential to avoid the loss of proteins, ATP and other important molecules over a long time range, it could perhaps not be the main or only reason for the baseline solute concentration gradients to exist between the cytoplasm and the surrounding medium (Ling and Walton 1976, Ling 1988, Pollack 2003). The membrane could have more important roles, for instance in keeping the overall cell architecture, shape and integrity in cooperation with the cytoskeleton scaffolding (see below) or managing the cellular interactions within the tissue. In this view, the physical properties of the cytoplasm itself are considered to support its own content. Clearly the properties of the protein–ion–water matrix gels which form the cytoplasm should have a key role which makes the cytoplasm radically different from a banal aqueous solution with free diffusing solutes.

The role of water

The fact that the cytoplasm content remains largely intact although the cell membrane has been disrupted (Kellermayer *et al* 1986) without any doubts indicates that some strong attractive forces must exist within the cytoplasm, which maintain its cohesion and prevent its water and content from leaking out. The roots of these forces can be found in a particular water phase or structure which results from the interactions between the negatively charged surfaces of cytoplasm proteins and the dipolar water molecules.

Liquid water physics. Life on Earth depends on the unusual structure of liquid water and its interaction with biological molecules. However, despite much work, many of the properties of water are still puzzling. Water's composition (two parts hydrogen, one part oxygen) was discovered by the London scientist Henry Cavendish in about 1781. Since then, decades of computer simulation studies on water and aqueous solutions have immensely broadened our knowledge about this molecule which still remains mysterious (see Finney (2004)) for a review). The water molecule comprises one heavy (oxygen) and two light (hydrogen) atoms. The O–H distance is slightly less than 1 Å and the HOH angle of its average geometry is around $104.52°$ ($105.5°$ in liquid water (Silvestrelli and Parrinello 1999), close to both a tetrahedral and a pentagon angle (Benedict *et al* 1956), but not quite, which gives the water molecule its particular geometry and unique properties. The water molecule, which is clearly not a sphere, has a global size of 3.2 Å (figure 5).
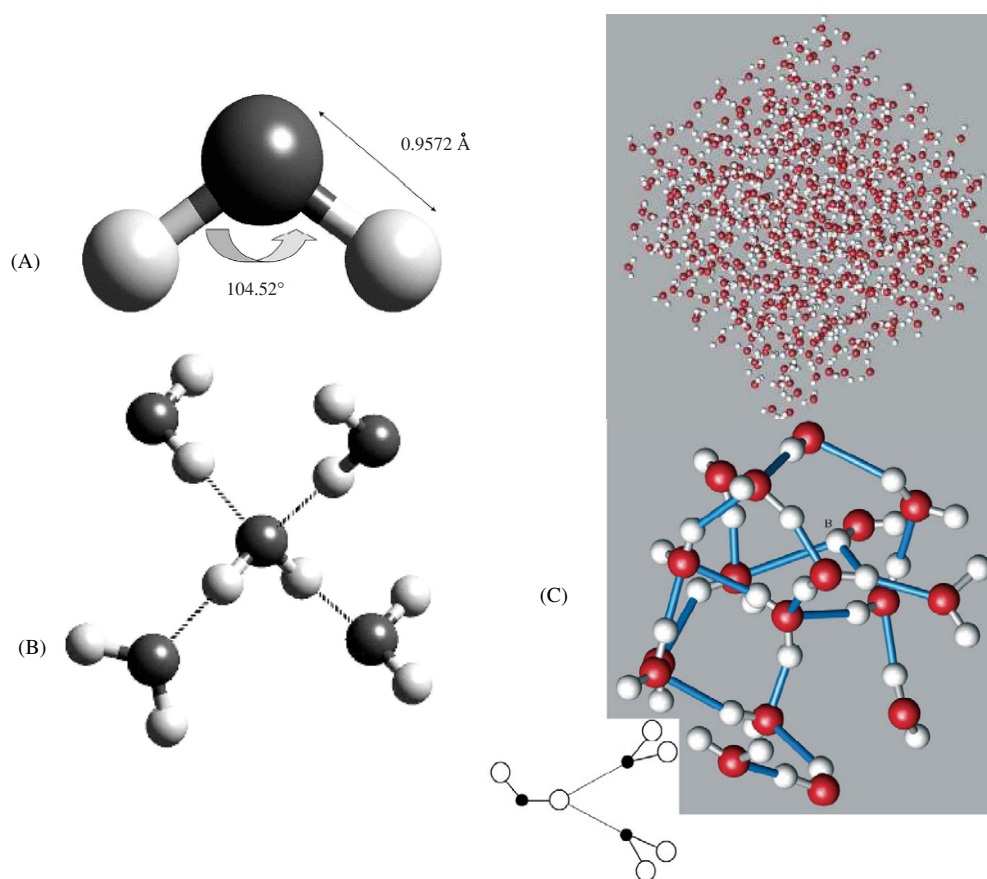
Figure 5. The water molecule. (A) Average geometry of the water molecule. (B) Four-coordinated water molecule showing the classic tetrahedral arrangement of the first-neighbour environment of a water molecule hydrogen bonding to four neighbours. The central molecule 'donates' two hydrogen bonds to its lower neighbours and 'accepts' a hydrogen bond from each of its two upper neighbours. (C) Top: snapshot of liquid water at 298 K. Bottom: close-up indicating likely hydrogen bonds between neighbouring molecules. Note the existence of both four- and three-coordinated molecules, as well as bifurcated interaction (B) in which one hydrogen apparently donates to two neighbouring lone pair regions (inset). Reprinted with permission from the publisher from Finney (2004).

This geometry is, however, only an average as the molecule is never static, but subject to several modes of vibrational motion. Another special feature is its charge distribution: the two positively and two negatively (Levis) charged regions separated by 0.061 nm classically form a tetrahedral symmetry which results in an important dipole moment with a high polarizability (up to 50% enhanced dipole moment in liquid water (Finney 2004)). Water molecules interact with each other through hydrogen bonding, as discovered in 1920 by Latimer and Robebush. The strength of this interaction is notably high ($20\,\mathrm{kJ\,mol^{-1}}$), well above thermal fluctuations at ambient temperatures, explaining why water is liquid in spite of the small size of its molecules. Furthermore, each water molecule can bind to four first-neighbours from its four charged sites (two donating and two accepting hydrogen bonds) forming a tetrahedral arrangement (figure 5). This geometry is critical, although this tetrahedral network is not

perfect in liquid water: while the four-coordination motif with 'linear' hydrogen bonds is the dominant configuration, there are significant local defects where the coordination is either greater or less than four with 'bifurcated' hydrogen bonds (Vuilleumier and Borgis 2006), which introduce local environment variability and prevent any long-range order, as expected in a liquid.

Diffusion of protons in liquid water does not occur via hydrodynamic Stokes diffusion of a rigid complex, but via a migration through the continual interconversion between covalent and hydrogen bonds throughout the water network. The classical view of proton mobility in water was the so-called Grotthuss mechanism (von Grotthuss 1806): a proton from a H_3O^+ ion moves rapidly along a hydrogen bond to a neighbouring water molecule, recreating a new H_3O^+ ion. A proton from this newly formed H_3O^+ ion similarly translocates to a neighbour water molecule, and so on. Unfortunately, experimental data do not fit well with this model (Lapid *et al* 2005). Proton mobility in water is too high and the water diffusion coefficient is anomalously too fast: proton hopping times between water molecules, as seen through NMR, are about 1.5 to 2 ps, while the mean time for a water molecule to move a distance of about one molecular diameter is 7 ps (Denisov and Halle 1996), well too short to be explained by the breaking of two or more hydrogen bonds required for a molecule to move. It has been suggested that the hydrogen-bond defects in the four-coordinated network account for the high mobility of water molecules and protons (Texeira *et al* 1985, Sciortino *et al* 1991) (Vuilleumier and Borgis 1999, Prielmeier *et al* 1987). Results from simulations using supercomputers have given reasonable hopping times by modelling local forces and quantum effects (such as proton tunnelling). A recent model (Marx *et al* 1999) indicates that H_9O^{4+} defects are formed by coordination of a hydrated proton (H_3O^+) with three neighbouring water molecules. The proton migrates by the (thermally induced) hydrogen-bond breaking in the second solvation shell of the H_3O^+ and subsequently forms a transient H_5O^{2+} complex where the proton is equally shared between two water molecules (figure 5) before finally binding to form a new H_9O^{4+} complex. The structural 'defect' is then displaced over a distance of about two water molecules (5 Å), while each particle does not move more than a fraction of 1 Å. An important consequence relevant to biology, of this network 'defect' model, as will be seen later, in that in liquid water, in contrast to other liquids, an *increase of structural order* of the liquid leads to a reduced density and *decreased diffusion mobility*, as the number of network defects declines (Sciortino *et al* 1991, 1992).

In summary, liquid water is not homogeneous at the nanoscopic level. Water molecules form in liquid water an infinite network of clusters with differing degrees of hydrogen bonding and tetrahedrality. The peculiar nature of those hydrogen bonds makes water as we know it, as their strength is just right within a narrow window of its ideal suitability for life: if the hydrogen bond strength was slightly different from its actual value then there would be considerable consequences for life.

Cellular water and polar interfaces. It is now widely accepted that cell water largely differs from bulk water and is not just a structureless, space-filling background medium where biological events occur. Physical properties of cell water drastically differ from bulk liquid water and ice: temperatures well below zero are needed for the cell water to freeze (Mazur 1970, Tanghe *et al* 2006) and cell water viscosity is very high (Luby-Phelps *et al* 1986, Bausch *et al* 1999, Wang *et al* 1993). Indeed, liquid water may also form other types of three-dimensional arrays in the presence of interfaces with charged materials. In such 'structured' water hydrogen bonds are also 'bent' (Sciortino *et al* 1991, 1992) to allow a different organization of the water molecules. With hydrophobic materials water molecules undergo an extensive self-association into 'clathrates' networks (Schrade *et al* 2001). In the

case of hydrophilic materials strong interactions with polarized water molecules arise and the water molecules become organized into layers. In cells, proteins have an especially profound effect on water due the presence of their charge which results in protein-water adsorption (Toney *et al* 1994, Pauling 1945). Protein charges orient the dipolar water molecules in a first layer, which, in turn, may orient other water molecules in successive layers in a cooperative manner (Ling 1965, Ling *et al* 1967). Although the multi-layer polarization model (Ling *et al* 1973, Ling and Walton 1976, Ling 1977) has remained extremely controversial in the physiology community (mainly because it put into question the role of the cell membrane, but also because it seemed inconsistent with beliefs accepted by the majority of the scientific community; see below), the presence of such structured water in cells has been now broadly confirmed (Clegg 1984b, Cameron *et al* 1997, Ling 2003). Depending on the mechanisms of water protein–surface interactions and the interaction distance (the influence seems to decay exponentially as a function of distance) different vocabularies have been used, such as 'bound', 'hydration', 'vicinal' or 'interfacial' water (Clegg 1984b, Wiggins 1990). It is generally considered that Van der Waals forces account for only one or two layers of water molecules at the protein surface (0.4 g/g water/protein covering 13% or more of the protein surface), but hydration water could represent much more *inside cells* (Rorschach *et al* 1991), up to about 2 to 4 g/g (dry weight) (Wiggins 1990), which represents 70 to 80% of cell mass or volume. Hence, water structuring and related effects on water mobility could well extend several water molecule layers away from the protein surface, perhaps as much as 50 Å (Clegg 1984a). Another explanation would be that the amounts of the first layers of interfacial water on internal proteins are larger than expected, up to 1.6 g/g in a collagen model (Fullerton and Amurao 2006). Water diffusion in the 5 Å thick hydration shell has been found to be around $0.5 \times 10^{-3} \ \mathrm{mm^2 \ s^{-1}}$ at 25 °C and shown to result from a stronger hydrogen-bonding structure than in bulk water (Steinhoff *et al* 1993).

Given the high degree of macromolecular packing in cytoplasm (surface-to-surface gaps between macromolecules are in the range of a new nanometres) and the exchange between water pools, one may consider that at least a substantial fraction if not all of its water content is structured, although perhaps to various degrees. A study in plant cells showed 30% of water molecules greatly reduced in mobility, 70% to a lesser extent, and essentially no bulk water (Pissis *et al* 1987). This water adsorption by the hydrophilic protein matrix gives the cytoplasm the structure of a gel which retains its water and its volume. Structured water also contributes to slow intracellular diffusion in addition to the presence of obstacles (Gershon *et al* 1985), as the hydrogen bonding defects are reduced and less efficient for proton mobility. Diffusion rates of solutes, such as high-energy phosphates (Yoshizaki *et al* 1982, Hubley *et al* 1995) or proteins (Wojcieszyn *et al* 1981) are also much reduced.

Another implication of the presence of structured water in cells is that the solubility of the solutes in cell water will change, because of the decreased availability of the hydrogen bonds: only small solutes will be able to penetrate the structured water network, while the others will be excluded (Ling 1993). For ions to penetrate the water network, the hydrated size (shell of structured water around the ion) must be considered, according to the classical Hofmeister series (Hofmeister 1888):

$$Mg^{2+} > Ca^{2+} > Na^{+} > K^{+} > Cl^{-} > NO_3^{-}.$$
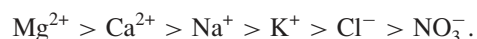
The largest ions are called 'structure promoting' or cosmotropic, whereas the smallest ones are called 'structure breaking' or chaotropic. Size-wise Na^+ and K^+ are on either size of a breakpoint (around 1.06 Å) between ion–water and water–water interactions (Collins 1995), so that ions, such as K^+ and Cl^- can penetrate the structured water network, while Na^+ is largely excluded (Ling 1993). In the cytoplasm K^+ and Cl^- get adsorbed onto the negatively

and positively charged sites of the macromolecules with a high affinity due to their water structure-breaking properties (Kellermayer *et al* 1986). Hence, the presence of structured water in the cytoplasm has been proposed as an alternative to cell membranes to explain the difference in ionic concentration between the cytoplasm and the extracellular compartment for Na^+ and K^+: hydrated Na^+ gets excluded, whereas K^+ accumulates within the cytoplasm and binds to the protein negative charges (Pollack 2003, Ling 1988). This, still debated, water-based ionic partition scheme would not require the presence of membranes (except for maintaining the water-structuring cellular protein content), nor energy demanding pumping mechanisms.

As for surfaces and membranes, recent and elegant physics studies have indeed confirmed that water polarization exists near charged surfaces and builds up considerable forces (Israelachvili and Wennerstrom 1996, Israelachvili and McGuiggan 1988, Horn and Israelachvili 1981, Grannick 1991). Through cooperative effects the protein trapping range has been reported to extend over distances up to 200 nm beyond physical surfaces, which accounts for up to hundreds of water molecule layers (Pashley and Kitchener 1979, Fisher *et al* 1981, Xu and Yeung 1998, Shelton 2000). The spatial extent of this water structuring process has not been established in biological tissues, but the reinforcement effects of the density and distribution of charges along a plane surface, particularly when the periodic pattern of positive and negative charges coincides with the dimensions of the structured water elementary blocks (about 16 Å) (Chou 1992), could help propagate the structuring effect on water molecules beyond several layers. Recent studies have pointed out the importance of the hydration process on the structure and function of biological membranes (headgroup and acyl chain motion (Pissis *et al* 1987)), but, in turn, membranes deeply influence water behaviour. Measurements in phospholipid membrane models have revealed a strong interaction of the lipids and the membrane proteins with its first hydration layer resulting in a reduced water diffusion parallel to the surface membrane, about five times smaller than in free water (0.44×10^{-3} mm^2 s^{-1}) (Fitter *et al* 1999). The water diffusion coefficient varies according to the water content (0.12 to 0.4×10^{-3} mm^2 s^{-1} for water concentrations increasing from 4.9 to 18.6 mol water/lipid), which means that the diffusion coefficient is further reduced near the membrane surface (Wassall 1996). Diffusion parallel to the membrane is unrestricted, as it does not depend on the diffusion time. On the other hand, the water diffusion coefficient in this membrane-bound layer is highly anisotropic, with $D_{perpendicular}$ as low as 10^{-6} mm^2 s^{-1} in somewhat impermeable membranes, but higher when bilayer defects or channels are present.

Implication for water diffusion MRI: conceptual model

The non-Gaussian diffusion behaviour in brain tissue could well result from these strong interactions between water, proteins, phospholipids, etc within the cytoplasm and at the interface with membranes. For all the reasons detailed above, one might speculate that the ($\approx 70\%$) 'fast" diffusion pool would correspond to the tissue bulk water in fast exchange with the water hydration shell around proteins and macromolecules (whether in the intra- or the extracellular space (figure 6), although the contribution from the latter is probably much smaller), hence its reduced value ($D_{fast} \approx 1.2 \times 10^{-3}$ mm^2 s^{-1}) compared to free water ($D_{bulk} \approx 3.0 \times 10^{-3}$ mm^2 s^{-1} at 37 °C). Considering both protein obstruction and hydration effects (Colsenet *et al* 2005) one gets for D_{fast}

$$D_{fast} = D_{bulk}\{1/[1 - (1 - C_{hydr}/C_{bulk})\varphi]\}(1 - \beta\varphi)/(1 + \beta\varphi/2) \tag{3}$$

where $\beta = (C_{bulk} D_{bulk} - C_{hydr} D_{hydr})/(C_{bulk} D_{bulk} + C_{hydr} D_{hydr}/2)$, and D_{hydr} is the water diffusion coefficient in the ≈ 5 Å hydration layer ($D_{hydr} \approx 0.3$–0.5×10^{-3} mm^2 s^{-1}), C_{bulk} is
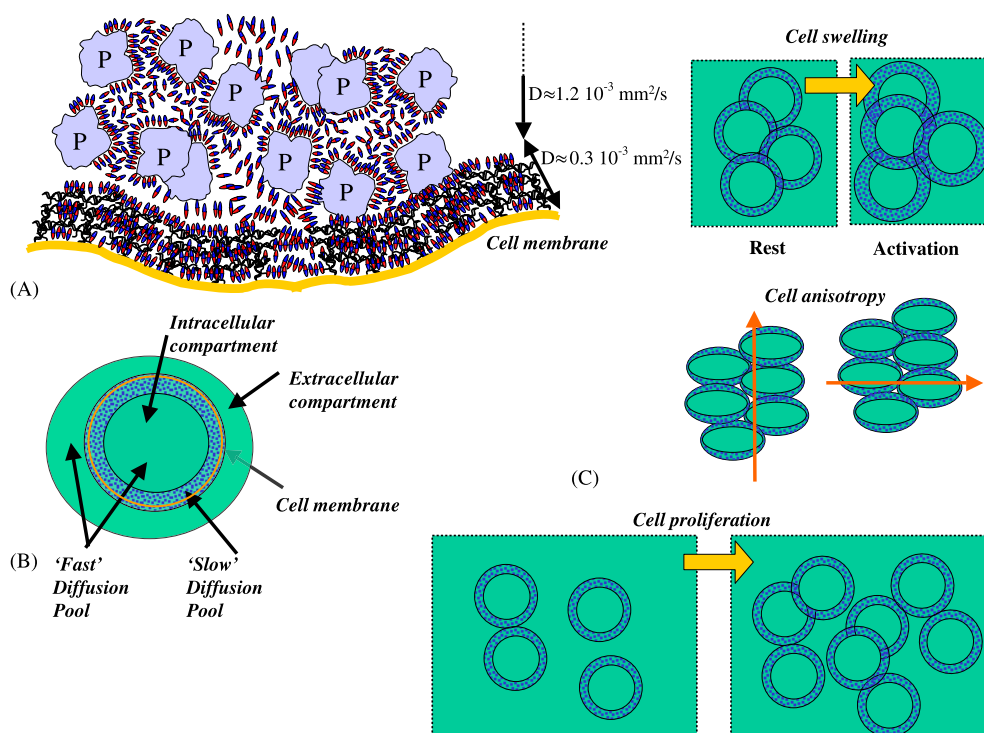
Figure 6. Membranes, water structure and diffusion. (A) Schematic representation of the structuring effect of charged proteins (P) and membranes on water molecules. Bulk water molecules are exchanging rapidly with the water molecules in the protein hydration shells. Other water molecules are trapped in a membrane-bound layer. Charges of the protein membranes and the underlying cytoskeleton strongly influence the water network in this layer, resulting in an increased order, a lower density and a slower diffusion coefficient. (B) Conceptual biphasic water diffusion model. The slow diffusion pool is made of a water layer trapped by the electrostatic forces of the protein membranes and associated cytoskeleton, as indicated in (A). The remaining of the water molecules, whether in the intra- or the extracellular compartment, constitutes the fast diffusion pool (which remains, however, slower that free water). (C) Diagram showing some predictions of the biphasic water diffusion model. Water diffusion would be reduced through an increase of the slow diffusion pool fraction associated with a membrane expansion, as during cell swelling (brain activation, top) or cell proliferation (cancer, bottom). It should be noted that MRI diffusion measurements are always performed along one particular direction. In most cases, tissues are isotropic. However, in tissues with anisotropic cells (middle), such as brain white matter, the number of membrane surface intersections with the measurement direction will vary according to the respective angle of the measurement direction and the long axis of the cells. The slow diffusion phase is, thus, expected to be the largest when those directions are perpendicular.

the concentration of the bulk water ($C_{bulk} = 1$ g cm^{-3}), C_{hydr} is the concentration of hydration water, and φ is the fractional volume occupied by proteins (which can be determined from the average cell protein mass, specific volume, ≈ 0.75 cm^3 g^{-1}, and shape). For spherical proteins one gets the expected value for D_{fast} with a water hydration around 1.6 g/g of protein, which is consistent with the literature (Fullerton and Amurao 2006).

As for the extracellular space experimental evidence suggests that it could be modelled as fluid-pores of 38–64 nm (Thorne and Nicholson 2006). While such pores are clearly hindering diffusion of TMA and dextrans (a few nanometres in diameter), they represent huge spaces for water molecules (3 Å in diameter). It is, therefore, not unconceivable that the

reduced value for water diffusion in the extracellular space mainly results from interactions with the extracellular matrix, rather than from geometric factors (pore size, topology) caused by obstructing cells (although this tortuosity component probably also partially contributes, in particular during ischaemia, as the pore size goes down to around 10 nm). This observation suggests why the extracellular water diffusion coefficient contributing to the FDP might not be so different than the intracellular FDP water diffusion coefficient, at least not enough to be separable with current diffusion MRI settings, because both share the same basic mechanisms of diffusion reduction, namely bulk water in fast exchange with the water hydration shell around macromolecules, although such macromolecules would dramatically differ in nature between the intra- and extracellular spaces. Tracers which are not bound to macromolecules and diffuse freely also have similar diffusion coefficients inside and outside cells (Duong *et al* 1998, 2001), but geometrical effects certainly contribute, as such tracers cannot cross cell membranes (restricted diffusion).

The ($\approx$30%) slow diffusion water pool would originate from packets of highly structured water molecules which are trapped within a membrane-bound water network and the three-dimensional cell microtrabecular network (Gershon *et al* 1985) (figure 6). The spatial distribution of charges at the membrane surface would result in an *increase of structural order* of water which leads to a reduced density and *decreased diffusion mobility*, as outlined above (Vuilleumier and Borgis 2006, Sciortino *et al* 1991). One should keep in mind that the cell membrane is not just a 10 nm bilayer with phospholipids and proteins. This membrane structuring effect could well be reinforced by the relatively thick and rigid matrix which runs contiguously and extends a few tens of nanometres on both sides of the membrane, the *glycocalyx* (made of tangled strands of glycoproteins) on the outside and the *cytoskeleton* (a dense polymer-gel matrix of cross-linked actin filaments and microtubules) on the inside. Hence, water structuring effects could occur undisturbed on relatively long ranges, because interstices within those networks are likely protein and ion free (Wiggins 1990, Clegg 1984a). Besides, as the membrane is not totally permeable, a fraction of water molecules 'bounce back' when hitting the membranes, which contributes to increasing their residence time within the layer. Both the SDP fraction ($\approx$30%) and its diffusion coefficient, D_{slow} ($\approx$0.3 $\times$ 10^{-3} mm^2 s^{-1}) agree well with literature values for this membrane interfacial structured water (Clegg 1984a, Fitter *et al* 1999, Pissis *et al* 1987).

In summary, the FDP and the SDP would correspond to two differently structured water pools, rather than specific water compartments. In the proposed model, both the SDP and FDP originate partly in the intracellular space and partly in the extracellular space. The presence of both a SDP and a FDP pools has, indeed, been found in an oocyte model (Sehy *et al* 2002b). Those two water pools are in slow or intermediate exchange and separable with current diffusion MRI settings (*b*-values, diffusion times) resulting in a biexponential diffusion decay behaviour. A more extensive model would require to take into account the residence time of water molecules within the SDP and FDP (intermediate exchange rate regime) using the Karger equations (Karger *et al* 1988) to allow for the SDP and FDP fractions to change slightly with the diffusion time.

Given the important surface/volume ratio of most cells, the cell membrane-bound water certainly constitutes an important fraction of the SDP. Under these conditions it might not be so surprising that any fluctuation in cell size, whether swelling or shrinking, would induce a large variation of the total membrane-bound water volume (the total cell membrane surface scales with the square of its radius), making diffusion-sensitized MRI, and especially its derived SDP fraction, very sensitive to cell size variations, as supported from the literature (Niendorf *et al* 1996, Benveniste *et al* 1992, OShea *et al* 2000, Hasegawa *et al* 1996, Dijkhuizen *et al* 1999, Van Der Toorn *et al* 1996).

To estimate the amount of water molecular interaction which would be necessary to account for the SDP volume, according to this membrane-bound water layer model, let us consider a very simple tissue model. This tissue is made of small spherical cells with an average radius R (e.g., 1 μm). On the other hand, only a fraction, p, of a MRI voxel volume, V, would be occupied by cells. For a compact volume optimally filled with spheres p is about 0.7. The number of cellular elements, N, per voxel is then

$$N/V = 3p/4\pi R^3. \tag{4}$$

On the other hand the total cell membrane surface in the voxel, S, is

$$S = 4\pi R^2 N. \tag{5}$$

Assuming that the SDP corresponds to a layer of water molecules which are trapped within a distance, ε, from the membranes, and a fixed volumic fraction, v_0, bound to the microtrabecular network and intracellular organelle membranes, such as mitochondria, and the endoplasmic reticulum, the slow volume fraction can be expressed as

$$V f_{slow} = (4\pi R^2 \varepsilon + 4\pi R^3 v_0/3)Nw \tag{6a}$$

or

$$f_{slow} = (3\varepsilon/R + v_0)/pw \tag{6b}$$

where w is the cell water total content (about 70–80%).

The membrane-bound water layer thickness can finally be estimated by

$$\varepsilon \cong (f_{slow}/pw - v_0)R/3. \tag{7}$$

Taking data from table 1 for f_{slow} and assuming that the membrane-bound water pool corresponds to 50% of the SDP ($v_0 = 0.5$) the estimated water layer thickness approaches 50 nm, i.e., about 25 nm on each side of the membrane.

According to this very simple, qualitative model, small variations in cell size or shape could affect the SDP fraction, as measured with diffusion MRI *at the voxel level* (not cellular level). This is because the changes in the SDP fraction must occur at the expense of the overall (intra- and extracellular) FDP fraction, if the number of cells per voxel, N, remains constant (i.e., p and 'tortuosity' must change). This mechanism would explain the apparent link between the water ADC and the extracellular space tortuosity; however, obstruction by cells would not be the prime effect.

Within a given cell the impact could be quite different, as the change of the *intracellular* fraction of the FDP (which scales with the cell volume) might offset the change in the *intracellular* SDP (which scales with the cell surface). Actually, no significant change in intracellular FDP and SDP could be observed in a swelling oocyte model (Sehy *et al* 2002b), but only a slight increase in the SDP and FDP diffusion coefficients, likely related to dilution effects within this giant cell.

Most clinical studies evaluate the ADC from two sets of images collected using two b-values, for instance $b = 0$ and $b = 1000$ s mm^{-2}. Under this condition the ADC, as determined from equation (1), would, in fact, correspond to

$$ADC = -\ln[f_{slow} \exp(-b\,D_{slow}) + f_{fast} \exp(-b\,D_{fast})]/b. \tag{8}$$

Using values from table 1 one gets ADC = 0.88 mm^2 s^{-1}, which is also very consistent with the literature. Drops in ADC in the order of 20–30% (up to 50% in animal models) are not uncommon during acute stroke. According to this model, assuming that almost all cell elements swell, the SDP should increase by 25–35%, which corresponds to a 16–22% increase in cell dimension (cytotoxic oedema). This model would also, at least qualitatively, explain

why the ADC is reduced in cancer or metastases. Because of the cell proliferation the density of membranes increases, as well as the membrane surface, and the related SDP volume in each voxel increases almost linearly with the number of cells per voxel (equation (6a)), resulting in a decreased ADC linked to cell proliferation. This hypothesis, if confirmed, would indicate that diffusion MRI should be more specific to cancer states than FDG-PET which relies on the unspecific increase of metabolism in cancer cells.

Another interesting prediction of this model is that the *volume* of the SDP would be *anisotropic* in oriented tissues, such as brain white matter, which is rather counterintuitive: the SDP fraction should be larger when diffusion measurements are made in a direction which maximizes membrane surface intersections, e.g., when diffusion is measured perpendicularly to white matter fibres: statistically, at the voxel level, water molecules which diffuse across cells will stay longer, on average during the diffusion time, in the membrane-bound layer than when diffusion is measured in the direction of the fibres. Hence, the SDP fraction is expected to increase and the FDP fraction to decrease (and D_{slow} to decrease further, in an intermediate exchange rate regime), but also because the diffusion coefficient in the membrane-bound layer is itself highly anisotropic (Fitter *et al* 1999). Conversely, the FDP fraction would increase (and the SDP fraction decrease) and D_{fast} increase for measurements in the direction of the fibres. This anisotropic effect in SDP and FDP volumes has, indeed, been observed in the human brain (Clark and Le Bihan 2000), as the SDP fraction in white matter varies between 10% and 50% from a measurement direction parallel to the fibres to a direction perpendicular to them.

Going back to the topic of this review and to the recent finding that water diffusion decreases during cortical activation (Le Bihan *et al* 2006), it has also been shown that this slowdown in diffusion solely reflects an increase in the SDP volume at the expense of the FDP. In view of the proposed conceptual model, this SDP volume inflation implies an extension of the membrane-bound water layer, hence membrane unfolding and cell swelling. Swelling of cell parts (e.g., dendrites or spines) or intracellular organelles (vesicles) could also lead to a similar observation, at least qualitatively.

At this stage, if it seems plausible to find mechanisms which explain how water diffusion could be reduced in tissues affected by cell swelling, it remains to be seen whether, why and how cells might swell during physiological activation. This is the topic of the following section.

Water and neuronal activation

The classical model of neuronal activation, built on the seminal observations of Hodgkin and Huxley in the early 1950s, rests mainly on the action potential which arises from discrete membrane-channel currents. In the action potential model activation triggers a flux of sodium down its concentration gradient through the membrane, which inverts the cell membrane potential. Potassium then flows out the cell, restoring its negative potential, while the sodium/potassium pumps restore the initial solute balance.

Yet, although sodium and potassium seem to play crucial roles, their absence does not prevent the action potential from occurring (Inoue *et al* 1973, Hagiwara *et al* 1964, Tasaki 1999). Hence, while in classical neurophysiology great importance was placed on transient electrical changes associated with the excitation processes, there is now compelling evidence that activation in nervous tissues is accompanied by other important physical phenomena and that the Hodgkin and Huxley model perhaps does not account for everything (Naundorf *et al* 2006).

Evidence for cell swelling upon activation

Structural changes in excited tissues have been observed, first from optical birefringence measurements (Cohen and Keynes 1968, Cohen *et al* 1968, Tasaki and Byrne 1993) and later more directly using piezoelectric transducers (Iwasa and Tasaki 1980, Iwasa *et al* 1980). Intrinsic optical imaging has revealed that in the brain cell swelling is one of the physiological responses associated with neuronal activation (Andrew and Macvicar 1994, Schwartzkroin *et al* 1998, Aitken *et al* 1999). In neural tissues these volume variations have been observed during both intense (Rothman 1985, Lux *et al* 1986, Meyer 1989, Holthoff and Witte 1998) and normal (Holthoff and Witte 1996, Takagi *et al* 2002) neuronal activation. Conversely, changes in blood osmolarity modify brain cortical excitability in animal models (Andrew *et al* 1989, Jefferys 1995, Dudek *et al* 1998, Schwartzkroin *et al* 1998) and in humans (Muller *et al* 2002). In the cat cortex transient changes in ionic transmembrane fluxes, especially K^+, are accompanied by the movement of water and cellular swelling partly due to osmotic imbalance (Manz *et al* 1999), while Cl^- influx through GABA-A receptors contributes to synaptically evoked cell swelling in hippocampus (Takagi *et al* 2002). Such swelling not only involves neuronal soma, but also focal areas along dendrites and axons (Takagi *et al* 2002, Inoue *et al* 2005), as well as glial cells (Macvicar and Hochman 1991, Macvicar *et al* 2002, Murase *et al* 1998, Holthoff and Witte 2000, Ransom *et al* 1985). Rat cortical neurons can recover from osmotic swelling only in the presence of an NMDA receptor antagonist (Churchwell *et al* 1996).

Hence, cortical cell swelling and its active regulation appear to have fundamental importance to neuronal function. Noticeably, these mechanical changes start simultaneously with the electric response with the peak of the mechanical response coinciding accurately with the action potential peak (Tasaki 1999, Tasaki and Iwasa 1982, Tasaki *et al* 1989). The response is asymmetric, as the swelling presents a sharp increase, while the return to baseline is smooth and monotonic (Tasaki 1999) (figure 7).

Interestingly, it has been recently discovered that pericytes around cortical capillaries could modulate locally the capillary diameter in the cortex upon brain activation, by changing their own shape (and size). Such variations in capillary diameter would be responsible for the rapid increase in blood volume which accompanies cortical activation (Lu *et al* 2005, Huppert *et al* 2006) and slightly later triggers an increase in blood flow from feeding arterioles (Peppiatt *et al* 2006). It remains to be seen whether changes in pericyte volume could also contribute to the changes observed with water diffusion MRI, but this observation would suggest another potential link between diffusion-based and haemodynamic (BOLD)-based fMRI signals.

Heat release and phase-transition

Another established process, first observed by Abott *et al* (1958) is a heat production concomitant to the action potential followed by partial (45–85%) reabsorption of the heat (Howarth *et al* 1968, 1979). Recent measurements made in the garfish olfactory nerves using synthetic pyroelectric polymers as heat sensors show that the thermal response also starts and peaks with the action potential resulting in a temperature rise by 23 $\mu°C$ (Tasaki *et al* 1989, Tasaki and Byrne 1987, 1991, Kusano and Tasaki 1990a, Tasaki and Iwasa 1981) (figure 6). Such heat release has also been observed during spreading depression (Tasaki and Byrne 1991). The combined observations of abrupt volume increase (swelling) and heat release suggest that a transient structural change, in the form of a physical first-order phase transition, occurs in the tissue during the generation of the action potential. However, rapid temperature changes, which may be much larger in magnitude than those implied by this proposed phase transition,
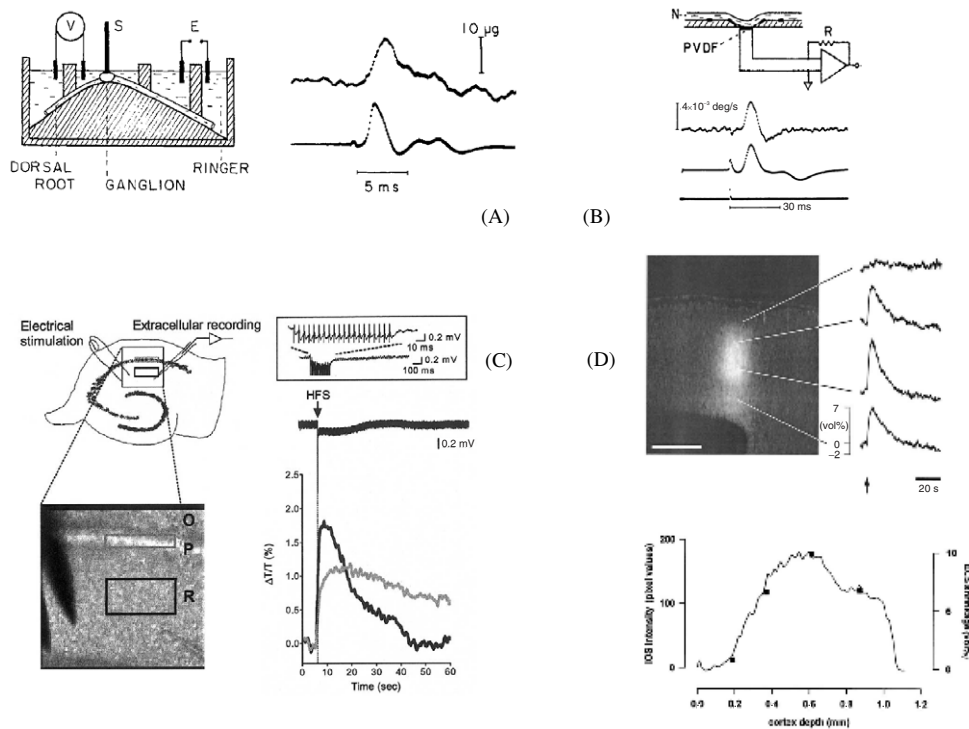
Figure 7. Cellular events accompanying activation. (A) Diagram of the set-up for recording mechanical responses of a dorsal root ganglion (S: stylus; E: stimulating electrode; V: input for recording the action potential). The plots show the mechanical response of the ganglion (top) and the associated action potential (bottom). Reprinted with permission from the publisher from Tasaki (1999). (B) Diagram of the set-up for recording thermal responses of garfish olfactory nerve (PVDF: thin pyroelectric film of polyvinylidene fluoride; R: feedback resistor of operational amplificatory). The plots show the action potential (top) and the thermal response (bottom) (horizontal bar: 30 ms; vertical bar: 4 degrees s^{-1}). Reprinted with permission from the publisher from Tasaki *et al* (1989). (C) Transient increases in near-infrared light (IR) transmittance in the rat hippocampal CA1 region. Left: experimental set-up and sample image (O: stratum oriens; P: stratum pyramidale; R: stratum radiatum). The black (dendritic region) and grey (somatic region) indicate areas for measurements. Right: traces from a single trial (top: extracellular field potential; bottom: IR transmittance changes). HFS indicates the time of high frequency stimulation. Reprinted with permission from the publisher from Takagi *et al* (2002). (D) Top: intrinsic optical signal (IOS) in rat brain slice 4 s after beginning of stimulation (pulses of 200 μs in a train of 50 Hz for 2 s) showing differential involvements within cortical layers (scale bar: 300 μm). The time course of the IOS and corresponding extracellular space shrinking is shown in different cortical layers. Bottom: intensity plot of the IOS and corresponding ECS shrinkage along the cortical depth. Reprinted with permission from the publisher from Holthoff and Witte (1998).

also arise from the biochemical reactions associated with neuronal activity, neuroenergetics and the kinetic design of excitatory synapses (Attwell and Gibb 2005). The concept that the action potential is an electrochemical manifestation of structural changes at the membrane surface rather than solely membrane electric changes is, indeed, not new (Williams 1970, Inoue *et al* 1973).

Mechanism of cortical cell swelling: water and the cytoskeleton

Ionic transmembrane shifts must be accompanied by water. However, osmotic changes linked only to fluxes of Na$^+$ and K$^+$ during the action potential cannot account quantitatively for the

observed volume changes (Tasaki and Byrne 1990). In the small non-myelinated fibres of the garfish olfactory nerves (0.2–0.3 μm) swelling is in the order of 2×10^{-2} μm^3. Such a large excitation-induced swelling, which has been observed in various nerve tissues, including mammalian ganglion cells (Kusano and Tasaki 1990b), cannot easily be ascribed to a simple translocation of water from the extra- to the intracellular compartment, but can be better explained by an overall decrease in the density of the excited tissue (Tasaki and Byrne 1990).

Further studies have identified that such non-electric effects, namely cell swelling and temperature increase in the excited tissue, take place mainly in a thin gel layer attached to the cell membrane and containing a high density of macromolecules, Ca^{2+} and structured water (Sato et al 1973, Tasaki and Byrne 1993, Tsukita et al 1986). This dense polymer–gel matrix of cross-linked actin filaments and microtubules runs contiguously to the cell membrane (Metuzals and Tasaki 1978, Endo et al 1979) with a high negative surface charge responsible for the baseline negative membrane potential (Tsukita et al 1986). It has been shown that agents which disrupt microtubules or solubilize gels, and thus eliminate this cytoskeleton, suppress the action potential (Tasaki et al 1965, Matsumoto et al 1979). Cytoskeletal integrity is necessary for the action potential to occur (Metuzals and Tasaki 1978).

Within this layer, structured water and Ca^{2+}/Na^+ cationic exchanges seem to play a crucial role (Tasaki and Byrne 1992b). The presence of calcium is vital, and its external concentration must be kept as a high level for the action potential to appear (Inoue et al 1973, Hagiwara et al 1964, Tasaki 1999). Calcium is a divalent cation and under baseline conditions has a sufficiently high concentration in the anionic gel cytoskeleton to maintain Ca^{2+} bridges which are formed between negative sites of the protein strands. The cytoskeleton polymer–gel matrix is kept condensed and the gel is very compact, as there is a cooperation effect between neighbouring anionic sites to form bridges (Tasaki 1999). During excitation the Na^+ concentration in the cytoskeleton sharply increases and Ca^{2+} is displaced by Na^+ in the anionic gel. As Na^+ is a monovalent cation binding disappears in a cooperative manner, and the matrix loosens and expands. This expansion, in turns, allows more Na^+ to enter and displace Ca^{2+}. In addition there is a massive movement and rearrangement (reordering) of water molecules around the exposed anionic charges of the unfolded proteins of the cytoskeleton and the cell membrane. Water dipoles build one upon another, wedging strands farther apart, which expose even more anionic sites, and so on. The cytoskeleton and attached membrane expands due to the enhancement of repulsive electrostatic forces between protein strands near the membrane, resulting in a swollen, lower-density structure with reduced diffusion (see above). The associated phase transition which necessarily accompanies such reordering of the water within the cell membrane-bound gel layer could be partially responsible for the liberation of heat which has been reported earlier. This process terminates, as covalent bonds within the cytoskeleton prevent further expansion, and the accumulation of cationic ions starts to neutralize anionic sites, competing against water structuring and finally triggering a reverse phase-transition of the membrane-layer water at the peak of the action potential: Na^+ is excluded from the cell, restoring the cell membrane potential, while Ca^{2+} recondenses the cytoskeleton.

Furthermore, these physical changes in the otherwise electrically charged cyotoskeleton could participate in the voltage transition observed in the action potential (Inoue et al 1973, Tasaki and Byrne 1994). At the end of the action potential the 'melting' of the structured water partially reabsorbs the released heat. Only the very large number of water molecules involved in the process could explain the level of observed changes, either in terms of swelling or heat release. Overall this cycling process with a spontaneous recovery is largely 'free' in terms of energy demand, although some energy would still be irreversibly lost in the process. This scheme is well supported by the observation of analogous transient swelling events in

synthetic negatively charged polymer gels containing both Na^+ and Ca^{2+} ions (Tasaki and Byrne 1992a, Tasaki 2005).

There is a further point of interest related to the heat release associated with the activation-induced phase transition. The substantial increased order in a water structure within the activated region, given the considerable number of water molecules involved, is associated with a decrease in entropy, $\Delta S < 0$. In order to offset this and to satisfy basic thermodynamic laws the activated region must give rise to a release of heat (loss of enthalpy, $\Delta H < 0$) and a rise in the temperature of the region, assuming that the system is isolated (no change in free energy, $\Delta G = 0$) during the very fast onset of activation (figure 7):

$$\Delta G = \Delta H - T \Delta S. \tag{9}$$

The restoration of the initial water status and return of cell volume to baseline, $\Delta S > 0$ would partially result from a reuptake of the heat and a production of internal energy ($\Delta H > 0$) through cell metabolism and membrane pump activation, which could occur at a slower pace (figure 7). It is widely supposed that one evolved function of the increase in blood flow accompanying local neuronal activity (which forms the bases of H_2O PET and BOLD fMRI) is to maintain temperature homeostasis (Collins et al 2004). Certainly this restricts temperature changes during activation to well below 0.1 °C. Overheating might adversely affect action potentials (Spyropolous 1961), although a mild fever of 1° celsius clearly has a limited impact on brain function. One group had already suggested that activation-induced changes in temperature could be at one origin of the vascular events detected by BOLD fMRI (Yablonskiy et al 2000), but the large temperature changes implied by this model have not been observed (Van Leeuwen et al 2000, Gorbach et al 2003).

Implications for functional neuroimaging

Cell swelling and the associated water phase-transitions, thus, seem to play a prominent role in the physiology of cell activation, and those phenomena have been put forward as a possible mechanism to explain the observed changes in water diffusion during brain activation (Le Bihan et al 2006). According to the biphasic diffusion model, (small) signal changes, dS/S, from the resting to the activated conditions can be formulated from equation (2) as

$$dS/S = (F_{slow} - F_{fast}) \, df_{slow} \tag{10}$$

where $F_{i = fast, slow} = \exp(-bD_i)/[f_{slow}\exp(-bD_{slow}) + f_{fast}\exp(-bD_{fast})]$ and df_i is the change in volume of the slow and fast diffusion pools resulting from activation (with $df_{fast} = -df_{slow}$). Variations of S_0, D_{slow} and D_{fast} were found to be of second order, as in Buckley et al (1999). Taking typical values for F_i and D_i (table 1), one gets with a b-value of 2400 s mm^{-2}

$$dS/S \cong 2.3 \, df_{slow}. \tag{11}$$

During activation of the human visual cortex changes on the order of $dS/S \cong 1.5\%$ and $df_{slow} \cong 0.65\%$ have been reported (Le Bihan et al 2006) (figure 8).

Let us now estimate how many cell elements should swell to produce those observed diffusion phase-transition changes, using the tissue model presented above (this model is, of course, extremely oversimplified, and does not represent the reality of the brain cortex with its many different components, neurons and glial cells, axons and dendrites, vessels and so on).

During activation, a fraction k of the cellular elements swell. Let us assume that each element experiences about the same radius increase, dR, upon activation (according to the literature, swelling would be around 10% in volume (Holthoff and Witte 1998)). From equation (6) and assuming that the number of cells per voxel, N/V, remains constant (which
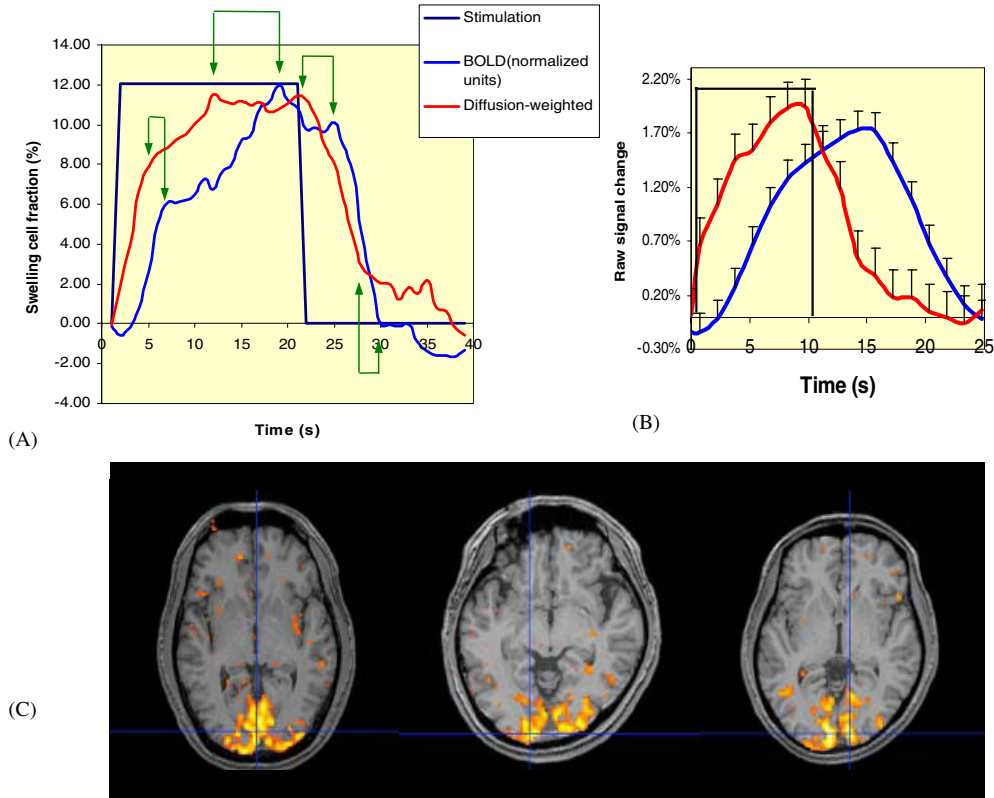
(A)

(B)

(C)

Figure 8. Diffusion fMRI. (A) Time course of the BOLD and diffusion fMRI responses in visual cortex (raw signal changes) for a 20 s stimulus and an image resolution of 3 s. Several landmarks can be seen on both curves, but the diffusion response comes always earlier than the BOLD response. Those landmarks could represent the activation of different neuronal clusters within the activated region. (B) Time course of the BOLD and diffusion fMRI responses in visual cortex (raw signal changes) for a 10 s stimulus and an image resolution of 2 s. The amplitude of the responses are comparable, but the diffusion response is clearly ahead of the BOLD response by several seconds, both at onset and offset. (C) Activation maps obtained with diffusion fMRI during visual stimulation in three subjects showing that the localization of the voxels where water diffusion is reduced are well localized within the brain cortex (courtesy D Le Bihan, S Urayama, T Aso, T Hanakawa and H Fukuyama, Human Brain Research Center, Kyoto University).

means that p increases slightly to compensate for the swelling), one obtains that the increase in the SPD fraction, df_{slow}, is

$$df_{slow} = 3kpw\,dR/R \qquad (12)$$

(in the calculation the extension of the cell radius is assumed to directly result from the expansion of the membrane/cytoskeleton-bound water layer, i.e., $d\varepsilon \cong dR$, and the intracellular amount of the SDP not linked to the membranes, $4\pi R^3 v_0/3$, is assumed to remain constant). Hence, taking the above figures, the observed 0.65% change in df_{slow} would only require about 15% of the elements in the voxel to swell by 4% in radius. Hence, only a small fraction of cells need to swell in order to be detected by diffusion MRI which would be an extremely sensitive functional neuroimaging tool, providing, of course, that the basic signal:noise ratio is not too low, which is, unfortunately, often the case with diffusion MRI, hence the aim for very high field MRI. The accidental peaks sometimes found along the time course of the SDP fraction could, perhaps, reflect the involvement of different cell

clusters in the cortical columns, which could be recruited and swell at different times during the activation (figure 8).

Conclusion

Water has been, so far, the molecule of choice for functional neuroimaging, whatever the modality, PET or MRI. This is clearly no accident given its ubiquitous distribution in living organisms and in the brain. Life cannot exist without liquid water, but it remains amazing that, although a great many number of theories have been published about the unusual physical properties of liquid water, sometimes with great controversy, we still do not understand the special relationship this tiny and apparently simple molecule has with our lives. The special features carried by the characteristics of water molecules are necessary for the operation of cellular biological mechanisms within cells, but, conversely, those mechanisms and the content of the cells have a profound impact on the water molecular structure itself, and this reciprocal relationship has often been overlooked in the past. Among those peculiar features is the molecular diffusion process of water. The mechanisms underlying water diffusion in itself at the molecular level are still a subject of research. However, here also life has given its imprint, as even this process, random by definition, seems to have been modified or even exploited in living organisms. Water diffusion in cells is different than in bulk water and reflects with great intimacy the subtle changes in water and cell structure which accompany various physiological and pathological states, hence the considerable success of diffusion MRI which can monitor such changes with accuracy in space and time.

So water may not just be a passive player in cell physiology. This is particularly true in the brain cortex where intricate biophysical mechanisms between membrane events and water movements and structure could take place during brain activation. Water diffusion has been found as a very early physiological surrogate marker of neuronal activation, which can be monitored to produce maps of cortical activation in the human brain with MRI. Many issues, though, have to be investigated to understand the actual mechanisms underlying the observed water diffusion changes. Although it appears that the swelling of a slow diffusion water phase could be linked to the expansion of a membrane-bound water layer upon activation-induced cell swelling, the physical nature of this slow diffusion water phase and the relationship between its volume variations and cell size changes, as well as the biophysical mechanisms underlying the observed swelling must be clarified. However, the possibility of observing transient cell swelling events in the brain of intact animals and humans would provide new opportunities to study the elementary processes underlying cortical activation and the existence of 'non-synaptic' mechanisms, as recently pointed out in animal models (Jefferys 1995, Dudek *et al* 1998) and in humans (Muller *et al* 2002). Such mechanisms could partly be responsible for the synchronized activation of neurons through changes in the size of the extracellular space (Jefferys 1995) and result in faster responses than synaptic mechanisms (Takagi *et al* 2002). Clearly, many questions remain without answers yet, but the aim of this review would be fully reached if it contributes to trigger some readers' interest in the puzzling interaction which could exist between the functioning of our brain and water, the 'molecule of the mind'.

References

Abbott B C, Hill A V and Howarth J V 1958 The positive and negative heat production associated with a single impulse *Proc. R. Soc. B*. **148** 149–87

Agre P 2005 Membrane water transport and aquaporins: looking back *Biol. Cell* **97** 355–56

Agre P, Nielsen S and Ottersen O P 2004 Towards a molecular understanding of water homeostasis in the brain *Neuroscience* **129** 849–50

Aitken P G, Fayuk D, Somjen G G and Turner D A 1999 Use of intrinsic optical signals to monitor physiological changes in brain tissue slices *Methods* **18** 91–103

Amiry-Moghaddam M and Ottersen O P 2003 The molecular basis of water transport in the brain *Nat. Rev. Neurosci.* **4** 991–1001

Andrew R D, Fagan M, Ballyk B A and Rosen B 1989 Seizure susceptibility and the osmotic state *Brain Res.* **498** 175–80

Andrew R D and Macvicar B A 1994 Imaging cell volume changes and neuronal excitation in the hippocampal slice *Neuroscience* **62** 371–83

Arrio-Dupont M, Foucault G, Vacher M, Devaux P F and Cribier S 2000 Translational diffusion of globular proteins in the cytoplasm of cultured muscle cells *Biophys. J.* **78** 901–7

Assaf Y and Cohen Y 1998 Non-mono-exponential attenuation of water and *N*-acetyl aspartate signals due to diffusion in brain tissue *J. Magn. Reson.* **131** 69–85

Assaf Y, Freidlin R Z, Rohde G K and Basser P J 2004 New modeling and experimental framework to characterize hindered and restricted water diffusion in brain white matter *Magn. Reson. Med.* **52** 965–78

Attwell D and Gibb A 2005 Neuroenergetics and the kinetic design of excitatory synapses *Nat. Rev. Neurosci.* **6** 841–49

Basser P J, Mattiello J and Le Bihan D 1994 MR diffusion tensor spectroscopy and imaging *Biophys. J.* **66** 259–67

Bausch A R, Moller W and Sackmann E 1999 Measurement of local viscoelasticity and forces in living cells by magnetic tweezers *Biophys. J.* **76** 573–79

Benedict W S, Gailar N and Plyler E K 1956 Rotational-vibration spectra in deuterated water vapour *J. Chem. Phys.* **24** 1139–65

Benveniste H, Hedlund L W and Johnson G A 1992 Mechanism of detection of acute cerebral ischemia in rats by diffusion-weighted magnetic resonance microscopy *Stroke* **23** 746–54

Boyle P J and Conway E J 1941 Potassium accumulation in muscle and associated changes *J. Cell Biol.* **20** 529–38

Bratton C B, Hopkins A L and Weinberg J W 1965 Nuclear Magnetic Resonance studies of living muscle *Science* **147** 738–9

Buckley D L, Bui J D, Phillips M I, Zelles T, Inglis B A, Plant H D and Blackband S J 1999 The effect of ouabain on water diffusion in the rat hippocampal slice measured by high resolution NMR imaging *Magn. Reson. Med.* **41** 137–42

Busch E, Gyngell M L, Eis M, Hoehn-Berlage M and Hossmann K-A 1996 Potassium-induced cortical spreading depressions during focal cerebral ischemia in rats: contribution to lesion growth assessed by diffusion-weighted NMR and biochemical imaging *J. Cereb. Blood Flow Metab.* **16** 1090–1099

Cameron I L, Hardman W E, Fullerton G D, Miseta A, Koszegi T, Ludany A and Kellermayer M 1996 Maintenance of ions, proteins and water in lens fiber cells before and after treatment with non-ionic detergents *Cell Biol. Int.* **20** 127–37

Cameron I L, Kanal K M, Keener C R and Fullerton G D 1997 A mechanistic view of the non-ideal osmotic and motional behavior of intracellular water *Cell Biol. Int.* **21** 99–13

Chang D C, Rorschach H E, Nichols B L and Hazlewood C F 1973 Implications of diffusion coefficient measurements for the structure of cellular water *Ann. NY Acad. Sci.* **204** 434–43

Chen K C and Nicholson C 2000 Changes in brain cell shape create residual extracellular space volume and explain tortuosity behavior during osmotic challenge *Proc. Natl Acad. Sci. USA* **97** 8306–11

Chin C L, Wehrli F W, Fan Y L, Hwang S N, Schwartz E D, Nissanov J and Hackney D B 2004 Assessment of axonal fiber tract architecture in excised rat spinal cord by localized NMR q-space imaging: simulations and experimental studies *Magn. Reson. Med.* **52** 733–40

Chou K C 1992 Energy-optimized structure of antifreeze proteins and its binding mechanism *J. Mol. Biol.* **223** 509–17

Churchwell K B, Wright S H, Emma F, Rosenberg P A and Strange K 1996 NMDA receptor activation inhibits neuronal volule regulation after swelling induced by veratridine-stimulated NA+ influx in rat cortical cultures *J. Neurosci.* **16** 7447–57

Clark C A and Le Bihan D 2000 Water diffusion compartmentation and anisotropy at high *b* values in the human brain *Magn. Reson. Med.* **44** 852–59

Clegg J S 1984a Properties and metabolism of the aqueous cytoplasm and its boundaries *Am. J. Physiol. Regul. Integr. Comp. Physiol.* **246** 133–51

Clegg J S 1984b Intracellular water and the cytomatrix: some methods of study and current views *J. Cell Biol.* **99** 167s–71s

Cohen L B and Keynes R D 1968 Evidence for structural changes during the action potential in nerves from the walking legs of Maia squinado *J. Physiol.* **194** 85–6P

Cohen L B, Keynes R D and Hille B 1968 Light scattering and birefringence changes during nerve activity *Nature* **218** 438–41

Cohen Y and Assaf Y 2002 High *b*-value q-space analyzed diffusion-weighted MRS and MRI in neuronal tissues—a technical review *NMR Biomed.* **15** 516–42

Collins K D 1995 Sticky ions in biological systems *Proc. Natl Acad. Sci. USA* **92** 5553–7

Collins C M, Smith M B and Turner R 2004 Model of local temperature changes in brain upon functional activation *J. Appl. Physiol.* **97** 2051–5

Colsenet R, Mariette F and Cambert M 2005 NMR relaxation and water self-diffusion studies in whey protein solutions and gels *J. Agric. Food. Chem.* **53** 6784–90

Cooper R L, Chang D B, Young A C, Martin J and Ancker-Johnson B 1974 Restricted diffusion in biophysical systems *Biophys. J.* **14** 161–77

Cope F W 1969 Nuclear magnetic resonance evidence using D2O for structured water in muscle and brain *Biophys. J.* **9** 303–19

Darquie A, Poline J B, Poupon C, Saint-Jalmes H and Le Bihan D 2001 Transient decrease in water diffusion observed in human occipital cortex during visual stimulation *Proc. Natl Acad. Sci. USA* **98** 9391–5

Denisov V P and Halle B 1996 Protein hydration dynamics in aqueous solution *Faraday Discuss.* **103** 227–44

Dietzel I, Heinemann U, Hofmeijer G and Lux H D 1980 Transient changes in the size of the extracellular space in the sensorimotor cortex of cats in relation to stimulus-induced changes in potassium concentration *Exp. Brain Res.* **40** 432–9

Dijkhuizen R M, de Graaf R A, Tulleken K A F and Nicolay K 1999 Changes in the diffusion of water and intracellular metabolites after excitotoxic injury and global ischemia in neonatal rat brain *J. Cereb. Blood Flow Metab.* **19** 341–9

Douek P, Turner R, Pekar J, Patronas N J and Le Bihan D 1991 MR color mapping of myelin fiber orientation *J. Comput. Assist. Tomogr.* **15** 923–9

Dudek F E, Yasumura T and Rash J E 1998 'Non-synaptic' mechanisms in seizures and epileptogenesis *Cell Biol. Int.* **22** 793–805

Duong T Q, Ackerman J J, Ying H S and Neil J J 1998 Evaluation of extra- and intracellular apparent diffusion in normal and globally ischemic rat brain via 19F NMR *Magn. Reson. Med.* **40** 1–13

Duong T Q, Sehy J V, Yablonskiy D A, Snider B J, Ackerman J J H and Neil J J 2001 Extracellular apparent diffusion in the rat brain *Magn. Reson. Med.* **45** 801–10

Einstein A 1956 (collection of papers translated from the German) *Investigations on the Theory of Brownian Motion* ed R Furthe and A D Cowper (New York: Dover)

Endo S, Sakai H and Matsumoto G 1979 Microtubules in squid giant axon *Cell Struct. Funct.* **4** 285–93

Finney J L 2004 Water? What's so special about it? *Phil. Trans. R.* B **359** 1145–63

Fisher I R, Gamble R A and Middlehurst J 1981 The Kelvin equation and the condensation of water *Nature* **290** 575–6

Fitter J, Lechner R E and Dencher N A 1999 Interactions of hydration water and biological membranes studied by neutron scattering *J. Phys. Chem.* B **103** 8036–50

Fox P T, Mintun M A, Raichle M E, Miezin F M, Allman J M and Van Essen D C 1986 Mapping human visual cortex with positron emission tomography *Nature* **323** 806–9

Fullerton G D and Amurao M R 2006 Evidence that collagen and tendon have monolayer water coverage in the native state *Cell Biol. Int.* **30** 56–65

Fullerton G D, Kanal K M and Cameron I L 2006 On the osmotically unresponsive water compartment in cells *Cell Biol. Int.* **30** 74–7

Garcia-Perez A I, Lopez-Beltran E A, Kluner P, Luque J, Ballesteros P and Cerdan S 1999 Molecular crowding and viscosity as determinants of translational diffusion of metabolites in subcellular organelles *Arch. Biochem. Biophys.* **362** 329–38

Gershon N D, Porter K R and Trus B L 1985 The cytoplasmic matrix: its volume and surface area and the diffusion of molecules through it *Proc. Natl Acad. Sci. USA* **82** 5030–34

Glynn I M 2002 A hundred years of sodium pumping *Annu. Rev. Physiol.* **64** 1–18

Gorbach A M, Heiss J, Kufta C, Sato S, Fedio P, Kammerer W A, Solomon J and Oldfield E H 2003 Intraoperative infrared functional imaging of human brain *Ann. Neurol.* **54** 297–309

Grannick S 1991 Motions and relaxations of confined liquids *Science* **253** 1374–9

Hagiwara S, Chichibu S and Naka K-i 1964 The effects of various ions on resting and spike potentials of barnacke muscle fibers *J. Gen. Physiol.* **48** 163–79

Hansen A J and Olsen C E 1980 Brain extracellular space during spreading depression and ischemia *Acta. Physiol. Scand.* **108** 355–65

Hasegawa Y, Formato J E, Latour L L, Gutierrez J A, Liu K F, Garcia J H, Sotak C H and Fisher M 1996 Severe transient hypoglycemia causes reversible change in the apparent diffusion coefficient of water *Stroke* **27** 1648–55

Hasegawa Y, Latour L L, Formato J E, Sotak C H and Fisher M 1995 Spreading waves of a reduced diffusion coefficient of water in normal and ischemic rat brain *J. Cereb. Blood Flow Metab.* **15** 179–87

Hazlewood C F, Rorschach H E and Lin C 1991 Diffusion of water in tissues and MRI *Magn. Reson. Med.* **19** 214–6

Hofmeister F 1888 Zur lehre von der wirkung der salze *Arch. Exp. Pathol. Pharmakol.* **24** 247–60

Holthoff K and Witte O W 1996 Intrinsic optical signals in rat neocortical slices measured with near-infrared dark-field microscopy reveal changes in extracellular space *J. Neurosci.* **16** 2740–9

Holthoff K and Witte O W 1998 Intrinsic optical signals in vitro: a tool to measure alterations in extracellular space with two-dimensional resolution *Brain Res. Bull.* **47** 649–55

Holthoff K and Witte O W 2000 Directed spatial potassium redistribution in rat neocortex *Glia* **29** 288–92

Horn R G and Israelachvili J 1981 Direct measurement of structural forces between two surfaces in a nonpolar liquid *J. Chem. Phys.* **75** 1400–11

Howarth J V, Keynes R D and Ritchie J M 1968 The origin of the initial heat associated with a single impulse in mammalian non-myelinated nerve fibres *J. Physiol.* **194** 745–93

Howarth J V, Ritchie J M and Stagg D 1979 The initial heat production in garfish olfactory nerve fibres *Proc. R. Soc.* B **205** 347–67

Hubley M J, Rosanske R C and Moerland T S 1995 Diffusion coefficients of ATP and creatine phosphate in isolated muscle: pulsed gradient 31P NMR of small biological samples *NMR Biomed.* **8** 72–8

Huppert T J, Hoge R D, Diamond S G, Franceschini M A and Boas D A 2006 A temporal comparison of BOLD, ASL, and NIRS hemodynamic responses to motor stimuli in adult humans *Neuroimage* **29** 368–82

Ide M 2006 Cancer screening with FDG-PET *Q. J. Nucl. Med. Mol. Imaging* **50** 23–7

Inoue H, Mori Si, Morishima S and Okada Y 2005 Volume-sensitive chloride channels in mouse cortical neurons: characterization and role in volume regulation *Eur. J. Neurosci.* **21** 1648–58

Inoue I, Kobatake Y and Tasaki I 1973 Excitability, instability and phase transitions in squid axon membrane under internal perfusion with dilute salt solutions *Biochim. Biophys. Acta* **307** 471–7

Israelachvili J and Wennerstrom H 1996 Role of hydration and water structure in biological and colloidal interactions *Nature* **379** 219–25

Israelachvili J N and McGuiggan P M 1988 Forces between surfaces in liquids *Science* **241** 795–800

Iwasa K and Tasaki I 1980 Mechanical changes in squid giant axons associated with production of action potentials *Biochem. Biophys. Res. Commun.* **95** 1328–31

Iwasa K, Tasaki I and Gibbons R C 1980 Swelling of nerve fibers associated with action potentials *Science* **210** 338–9

Jefferys J G R 1995 Nonsynaptic modulation of neuronal activity in the brain: electrical currents and extracellular ions *Physiol. Rev.* **75** 689–715

Karger J, Pfeifer H and Heink W 1988 Principles and application of self-diffusion measurements by nuclear magnetic resonance *Adv. Magn. Reson.* **12** 1–89

Kasturi S R, Chang D C and Hazlewood C F 1980 Study of anisotropy in nuclear magnetic resonance relaxation times of water protons in skeletal muscle *Biophys. J.* **30** 369–81

Kellermayer M, Ludany A, Jobst K, Szucs G, Trombitas K and Hazlewood C F 1986 Cocompartmentation of proteins and K+ within the living cell *Proc. Natl Acad. Sci. USA* **83** 1011–5

Kroenke C D, Ackerman J J H and Yablonskiy D A 2004 On the nature of the NAA diffusion attenuated MR signal in the central nervous system *Magn. Reson. Med.* **52** 1052–59

Kusano K and Tasaki I 1990a Heat generation associated with synaptic transmission in the mammalian superior cervical ganglion *J. Neurosci. Res.* **25** 249–55

Kusano K and Tasaki I 1990b Mechanical changes associated with synaptic transmission in the mammalian superior cervical ganglion *J. Neurosci. Res.* **25** 243–48

Kwong K K, Belliveau J W and Chesler D A 1992 Dynamic magnetic resonance imaging of human brain activity during primary sensory stimulation *Proc. Natl Acad. Sci. USA* **89** 5675–79

Lapid H, Agmon N, Petersen M K and Voth G A 2005 A bond-order analysis of the mechanism for hydrated proton mobility in liquid water *J. Chem. Phys.* **122** 14506

Latour L L, Hasegawa Y, Formato J E, Fisher M and Sotak C H 1994a Spreading waves of decreased diffusion coefficient after cortical stimulation in the rat brain *Magn. Reson. Med.* **32** 189–98

Latour L L, Svoboda K, Mitra P P and Sotak C H 1994b Time-dependent diffusion of water in a biological model system *Proc. Natl Acad. Sci.* **91** 1229–33

Le Bihan D 1995 Molecular diffusion, tissue microdynamics and microstructure *NMR Biomed.* **8** 375–86

Le Bihan D 2003 Looking into the functional architecture of the brain with diffusion MRI *Nat. Rev. Neurosci.* **4** 469–80

Le Bihan D and Breton E 1985 Imagerie de diffusion *in vivo* par résonance magnétique nucléaire *C. R. Acad. Sci. Paris. T.* **301** Série II:1109–12

Le Bihan D, Breton E, Lallemand D, Grenier P, Cabanis E and Laval Jeantet M 1986 MR imaging of intravoxel incoherent motions: application to diffusion and perfusion in neurologic disorders *Radiology* **161** 401–7

Le Bihan D, Mangin J F, Poupon C, Clark C A, Pappata S and Molko N 2001 Diffusion tensor imaging: concepts and applications *J. Magn. Reson. Imaging* **13** 534–46

Le Bihan D, Turner R and Douek P 1993 Is water diffusion restricted in human brain white matter? An echo-planar NMR imaging study *Neuro. Rep.* **4** 887–90

Le Bihan D, Urayama S-i, Aso T, Hanakawa T and Fukuyama H 2006 Direct and fast detection of neuronal activation in the human brain with diffusion MRI *Proc. Natl Acad. Sci.* **103** 8263–68

LeBihan D and van Zijl P 2002 From the diffusion coefficient to the diffusion tensor *NMR Biomed.* **15** 431–34

Lehericy S *et al* 2002 Arteriovenous brain malformations: is functional MR imaging reliable for studying language reorganization in patients? Initial observations *Radiology* **223** 672–82

Ling G N 1965 The physical state of water in living cell and model systems *Ann. NY Acad. Sci.* **125** 401–17

Ling G N 1977 The functions of polarized water and membrane lipids: a rebuttal *Physiol. Chem. Phys.* **9** 301–11

Ling G N 1988 A physical theory of the living state: application to water and solute distribution *Scanning Microsc.* **2** 899–913

Ling G N 1993 A quantitative theory of solute distribution in cell water according to molecular size *Physiol. Chem. Phys. Med. NMR* **25** 145–75

Ling G N 1997 Debunking the alleged resurrection of the sodium pump hypotheses *Physiol. Chem. Phys. Med. NMR* **29** 123–98

Ling G N 2003 A new theoretical foundation for the polarized-oriented multilayer theory of cell water and for inanimate systems demonstrating long-range dynamic structuring of water molecules *Physiol. Chem. Phys. Med. NMR* **35** 91–130

Ling G N, Miller C and Ochsenfeld M M 1973 The physical state of solutes and water in living cells according to the association-induction hypothesis *Ann. NY Acad. Sci.* **204** 6–50

Ling G N, Ochsenfeld M M and Karreman G 1967 Is the cell membrane a universal rate-limiting barrier to the movement of water between the living cell and its surrounding medium *J. Gen. Physiol.* **50** 1807–20

Ling G N and Walton C L 1976 What retains water in living cells *Science* **191** 293–95

Logothetis N K, Pauls J, Augath M, Trinath T and Oeltermann A 2001 Neurophysiological investigation of the basis of the fMRI signal *Nature* **412** 150–57

Logothetis N K and Wandell B A 2004 Interpreting the BOLD signal *Annu. Rev. Physiol.* **66** 735–69

Lu H, Soltysik D A, Ward B D and Hyde J S 2005 Temporal evolution of the CBV-fMRI signal to rat whisker stimulation of variable duration and intensity: a linearity analysis *Neuroimage* **26** 432–40

Luby-Phelps K, Taylor D L and Lanni F 1986 Probing the structure of cytoplasm *J. Cell Biol.* **102** 2015–22

Lux H D, Heinemann U and Dietzel I 1986 Ionic changes and alterations in the size of the extracellular space during epileptic activity *Adv. Neurol.* **44** 619–39

Macvicar B A, Feighan D, Brown A and Ransom B 2002 Intrinsic optical signals in the rat optic nerve: role for K+ uptake via NKCC1 and swelling of astrocytes *Glia* **37** 114–23

Macvicar B A and Hochman D 1991 Imaging of synaptically evoked intrinsic optical signals in hippocampal slices *J. Neurosci.* **11** 1458–69

Magistretti P J and Pellerin L 1999 Cellular mechanisms of brain energy metabolism and their relevance to functional brain imaging *Philos. Trans. R. Soc. B* **354** 1155–63

Maier S E, Bogner P, Bajzik G, Mamata H, Mamata Y, Repa I, Jolesz F A and Mulkern R V 2001 Normal brain and brain tumor: multicomponent apparent diffusion coefficient line scan imaging *Radiology* **219** 842–49

Mancuso A, Derugin N, Ono Y, Hara K, Sharp F R and Weinstein P R 1999 Transient MRI-detected water apparent diffusion coefficient reduction correlates with c-fos mRNA but not hsp70 mRNA induction during focal cerebral ischemia in rats *Brain Res.* **839** 7–22

Mangia S, Giove F, Bianciardi M, Di Salle F, Garreffa G and Maraviglia B 2003 Issues concerning the construction of a metabolic model for neuronal activation *J. Neurosci. Res.* **71** 463–67

Manz B, Chow P S and Gladden L F 1999 Echo-planar imaging of porous media with spatial resolution below 100 μm *J. Magn. Reson.* **136** 226–30

Marx D, Tuckerman M E, Hutter J and Parrinello M 1999 The nature of the hydrated excess proton in water *Nature* **397** 601–4

Matsumoto G, Kobayashi T and Sakai H 1979 Restoration of the excitability of squid giant axon by tubulin–tyrosine ligase and microtubule proteins *J. Biochem. (Tokyo)* **86** 1155–58

Mazur P 1970 Cryobiology: the freezing of biological systems *Science* **168** 939–49

Metuzals J and Tasaki I 1978 Subaxolemmal filamentous network in the giant nerve fiber of the squid (Loligo pealei L.) and its possible role in excitability *J. Cell Biol.* **78** 597–621

Meyer F B 1989 Calcium, neuronal hyperexcitability and ischemic injury *Brain Res. Rev.* **14** 227–43

Moonen C T W, Pekar J, De Vleeschouwer M H M, Van Gelderen P, Van Zijl P C M and Des Pres D 1991 Restricted and anisotropic displacement of water in healthy cat brain and in stroke studied by NMR diffusion imaging *Magn. Reson. Med.* **19** 327–32

Moseley M E, Cohen Y and Kucharczyk J 1990a Diffusion-weighted MR imaging of anisotropic water diffusion in cat central nervous system *Radiology* **176** 439–46

Moseley M E, Cohen Y and Mintorovitch J 1990b Early detection of regional cerebral ischemic injury in cats: evaluation of diffusion and T2-weighted MRI and spectroscopy *Magn. Reson. Med.* **14** 330–46

Mulkern R V *et al* 1999 Multi-component apparent diffusion coefficients in human brain *NMR Biol.* **12** 51–62

Muller V, Birbaumer N, Preissl H, Braun C and Lang F 2002 Effects of water on cortical excitability in humans *Eur. J. Neurosci.* **15** 528–38

Murase K, Saka T, Terao S, Ideka H and Asai T 1998 Slow intrinsic optical signals in the rat spinal cord dorsal horn slice *Neuro. Rep.* **9** 3663–7

Naundorf B, Wolf F and Volgushev M 2006 Unique features of action potential initiation in cortical neurons *Nature* **440** 1060–3

Nicholson C and Philipps J M 1981 Ion diffusion modified by tortuosity and volume fraction in the extracellular micorenvrionment of the rat cerebellum *J. Physiol.* **321** 225–57

Nicholson C and Sykova E 1998 Extracellular space structure revealed by diffusion analysis *Trends Neurosci.* **21** 207–15

Nicholson C and Tao L 1993 Hindered diffusion of high molecular weight compounds in brain extracellular microenvironment measured with integrative optical imaging *Biophys. J.* **65** 2277–90

Niendorf T, Dijkhuizen R M, Norris D G, Van Lookeren Campagne M and Nicolay K 1996 Biexponential diffusion attenuation in various states of brain tissue: implications for diffusion-weighted imaging *Magn. Reson. Med.* **36** 847–57

Norris D G, Niendorf T and Leibfritz D 1994 Healthly and infarcted brain tissues studied at short diffusion times: the origins of apparent restriction and the reduction in apparent diffusion coefficient *NMR Biomed.* **7** 304–10

Novikov E G, Van Dusschoten D and Van As H 1998 Modeling of self-diffusion and relaxation time NMR in multi-compartment systems *J. Magn. Reson.* **135** 522–8

Ogawa S, Menon R S, Tank D W, Kim S G, Merkle H, Ellermann J M and Ugurbil K 1993 Functional brain mapping by blood oxygenation level-dependent contrast magnetic resonance imaging: a comparison of signal characteristics with a biophysical model *Biophys. J.* **64** 803–8

O'Shea J M, Williams S R, van Bruggen N and GardnerMedwin A R 2000 Apparent diffusion coefficient and MR relaxation during osmotic manipulation in isolated turtle cerebellum *Magn. Reson. Med.* **44** 427–32

Pashley R M and Kitchener J A 1979 Surface forces in adsorbed multilayers of water on quartz *J. Coll. Interface Sci.* **71** 491–500

Pauling L 1945 The adsorption of water by proteins *J. Am. Chem. Soc.* **67** 555–7

Peppiatt C M, Howarth C, Mobbs P and Attwell D 2006 Bidirectional control of CNS capillary diameter by pericytes *Nature* **443** 700–4

Phillips J M and Nicholson C 1979 Anion permeability in spreading depression investigated with ion-sensitive microelectrodes *Brain Res.* **173** 567–71

Pissis P, Anagnostopoulou-Konsta A and Apekis L 1987 A dielectric study of the state of water in plant stems *J. Exp. Bot.* **38** 1528–40

Pollack G H 2001 Is the cell a gel—and why does it matter? *Japan. J. Physiol.* **51** 649–60

Pollack G H 2003 The role of aqueous interfaces in the cell *Adv. Coll. Interface Sci.* **103** 173–96

Posner M I, Peterson S E, Fox P T and Raichle M E 1988 Localization of cognitive operations in the human brain *Science* **240** 1627–31

Prielmeier F X, Lang E W, Speedy R J and Ludemann H 1987 Diffusion in supercooled water to 300 MPa *Phys. Rev. Lett.* **59** 1128–31

Raichle M E 1994 Visualizing the mind *Sci. Am.* **270** 58–64

Raichle M E and Mintun M A 2006 Brain work and brain imaging *Annu. Rev. Neurosci.* **29** 449–76

Ransom B R, Yamate C L and Connors B W 1985 Activity-dependent shrinkage of extracellular space in rat optic nerve: a developmental study *J. Neurosci.* **5** 532–35

Rorschach H E, Chang D C, Hazlewood C F and Nichols B L 1973 The diffusion of water in striated muscle *Ann. NY Acad. Sci.* **204** 445–52

Rorschach H E, Lin C and Hazlewood C F 1991 Diffusion of water in biological tissues *Scanning Microsc.* Suppl. 5 S1–S9

Rothman S M 1985 The neurotoxicity of excitatory amino acids is produced by passive chloride influx *J. Neurosci.* **5** 1483–9

Roy C W and Sherrington C S 1890 On the regulation of the blood supply of the brain *J. Physiol.* **11** 85–108

Röther J, De Crespigny A J, D'Arcueil H and Moseley M E 1996 MR detection of cortical spreading depression immediately after focal ischemia in the rat *J. Cereb. Blood Flow Metab.* **16** 214–21

Sato H, Tasaki I, Carbone E and Hallett M 1973 Changes in the axon birefringence associated with excitation: implications for the structure of the axon membrane *J. Mechanochem. Cell Motil.* **2** 209–17

Schrade P, Klein H, Egry I, Ademovic Z and Klee D 2001 Hydrophobic volume effects in albumin solutions *J. Coll. Interface Sci.* **234** 445–7

Schwartzkroin P A, Baraban S C and Hochman D W 1998 Osmolarity, ionic flux, and changes in brain excitability *Epilepsy Res.* **32** 275–85

Sciortino F, Geiger A and Stanley H E 1991 Effect of defects on molecular mobility in liquid water *Nature* **354** 218–21

Sciortino F, Geiger A and Stanley H E 1992 Network defects and molecular mobility in liquid water *J. Chem. Phys.* **96** 3857–65

Sehy J V, Ackerman J J H and Neil J J 2002a Apparent diffusion of water, ions, and small molecules in the Xenopus oocyte is consistent with Brownian displacement *Magn. Reson. Med.* **48** 42–51

Sehy J V, Ackerman J J H and Neil J J 2002b Evidence that both fast and slow water ADC components arise from intracellular space *Magn. Reson. Med.* **48** 765–70

Seksek O, Biwersi J and Verkman A S 1997 Translational diffusion of macromolecule-sized solutes in cytoplasm and nucleus *J. Cell Biol.* **138** 131–42

Shelton D P 2000 Collective molecular rotation in water and other simple liquids *Chem. Phys. Lett.* **325** 513–6

Siegel B A and Dehdashti F 2005 Oncologic PET/CT: current status and controversies *Eur. Radiol.* **15** (Suppl. 4) D127–32

Silvestrelli P L and Parrinello M 1999 Structural, electronic, and bonding properties of liquid water from first principles *J. Chem. Phys.* **111** 3572–80

Sotak C H 2002 The role of diffusion tensor imaging in the evaluation of ischemic brain injury—a review *NMR Biomed.* **15** 561–9

Sotak C H 2004 Nuclear magnetic resonance (NMR) measurement of the apparent diffusion coefficient (ADC) of tissue water and its relationship to cell volume changes in pathological states *Neurochem. Int.* **45** 569–82

Spyropolous C S 1961 Initiation and abolition of electric response by thermal and chemical means *Am. J. Physiol.* **200** 203–8

Stanisz G J, Szafer A, Wright G A and Henkelman R M 1997 An analytical model of restricted diffusion in bovine optic nerve *Magn. Reson. Med.* **37** 103–11

Steinhoff H J, Kramm B, Hess G, Owerdieck C and Redhardt A 1993 Rotational and translational water diffusion in the hemoglobin hydration shell: dielectric and proton nuclear relaxation measurements *Biophys. J.* **65** 1486–95

Sukstanskii A L, Yablonskiy D A and Ackerman J J H 2004 Effects of permeable boundaries on the diffusion-attenuated MR signal: insights from a one-dimensional model *J. Magn. Reson.* **170** 56–66

Takagi S, Obata K and Tsubokawa H 2002 GABAergic input contributes to activity-dependent change in cell volume in the hippocampal CA1 region *Neurosci. Res.* **44** 315–24

Takahara T, Imai Y, Yamashita T, Yasuda S, Nasu S and van Cauteren M 2004 Diffusion-weighted whole-body imaging with background body signal suppression (DWIBS): technical improvement using free breathing, STIR and high-resolution 3D display *Radiat. Med.* **22** 275–82

Tanghe A, Van Dijck P and Thevelein J M 2006 Why do microorganisms have aquaporins? *Trends Microbiol.* **14** 78–85

Tanner J E 1978 Transient diffusion in a system partitioned by permeable barriers: application to NMR measurements with a pulsed field gradient *J. Chem. Phys.* **69** 1748–54

Tanner J E 1979 Self diffusion of water in frog muscle *Biophys. J.* **28** 107–16

Tasaki I 1999 Rapid structural changes in nerve fibers and cells associated with their excitation processes *Japan. J. Physiol.* **49** 125–38

Tasaki I 2005 Repetitive abrupt structural changes in polyanionic gels: a comparison with analogous processes in nerve fibers *J. Theor. Biol.* **236** 2–11

Tasaki I and Byrne P M 1987 Heat production associated with synaptic transmission in the bullfrog spinal cord *Brain Res.* **407** 386–9

Tasaki I and Byrne P M 1990 Volume expansion of nonmyelinated nerve fibers during impulse conduction *Biophys. J.* **57** 633–5

Tasaki I and Byrne P M 1991 Demonstration of heat production associated with spreading depression in the amphibian retina *Biochem. Biophys. Res. Commun.* **174** 293–7

Tasaki I and Byrne P M 1992a Discontinuous volume transitions in ionic gels and their possible involvement in the nerve excitation process *Biopolymers* **32** 1019–23

Tasaki I and Byrne P M 1992b Rapid structural changes in nerve fibers evoked by electric current pulses *Biochem. Biophys. Res. Commun.* **188** 559–64

Tasaki I and Byrne P M 1993 The origin of rapid changes in birefringence, light scattering and dye absorbance associated with excitation of nerve fibers *Japan. J. Physiol.* **43** (Suppl. 1) S67–75

Tasaki I and Byrne P M 1994 Optical changes during nerve excitation: interpretation on the basis of rapid structural changes in the superficial gel layer of nerve fibers *Physiol. Chem. Phys. Med. NMR* **26** 101–10

Tasaki I and Iwasa K 1981 Temperature changes associated with nerve excitation: detection by using polyvinylidene fluoride film *Biochem. Biophys. Res. Commun.* **101** 172–6

Tasaki I and Iwasa K 1982 Further studies of rapid mechanical changes in squid giant axon associated with action potential production *Japan. J. Physiol.* **32** 505–18

Tasaki I, Kusano K and Byrne P M 1989 Rapid mechanical and thermal changes in the garfish olfactory nerve associated with a propagated impulse *Biophys. J.* **55** 1033–40

Tasaki I, Singer I and Takenaka T 1965 Effects of internal and external ionic environment on excitability of squid giant axon: a macromolecular approach *J. Gen. Physiol.* **48** 1095–123

Taylor D G and Bushell M C 1985 The spatial mapping of translational diffusion coefficients by the NMR imaging technique *Phys. Med. Biol.* **30** 345–9

Texeira J, Bellisent-Funel M-C, Chen S H and Dianoux A J 1985 Experimental determination of the nature of diffusive motions of water molecules at low temperature *Phys. Rev. A.* **31** 1913

Thorne R G and Nicholson C 2006 *In vivo* diffusion analysis with quantum dots and dextrans predicts the width of brain extracellular space *Proc. Natl Acad. Sci. USA* **103** 5567–72

Toney M F, Howard J R, Richer J, Borges G L, Gordon J G, Melroy O R, Wiesler D G, Yee D and Sorensen L B 1994 Voltage-dependent ordering of water molecules at an electrode-electrolyte interface *Nature* **368** 444–6

Trantham E C, Rorschach H E, Clegg J S, Hazlewood C F, Nicklow R M and Wakabayashi N 1984 Diffusive properties of water in Artemia cysts as determined from quasi-elastic neutron scattering spectra *Biophys. J.* **45** 927–38

Tsukita S, Tsukita S, Kobayashi T and Matsumoto G 1986 Subaxolemmal cytoskeleton in squid giant axon: II. Morphological identification of microtubule- and microfilament-associated domains of axolemma *J. Cell Biol.* **102** 1710–25

Turner R 2002 How much cortex can a vein drain? Downstream dilution of activation-related cerebral blood oxygenation changes *Neuroimage* **16** 1062–7

Van Der Toorn A, Sykova E, Dijkhuizen R M, Vorisek I, Vargova L, Skobisova E, Van Lookeren Campagne M, Reese T and Nicolay K 1996 Dynamic changes in water ADC, energy metabolism, extracellular space volume, and tortuosity in neonatal rat brain during global ischemia *Magn. Reson. Med.* **36** 52–60

Van Leeuwen G M, Hand J W, Kagendijk J J, Azzopardi D V and Edwards A D 2000 Numerical modeling of temperature distributions within the neonatal head *Pediatr. Res.* **48** 351–6

van der Weerd L, Melnikov S M, Vergeldt F J, Novikov E G and VanAs H 2002 Modelling of self-diffusion and relaxation time NMR in multicompartment systems with cylindrical geometry *J. Magn. Reson.* **156** 213–21

von Grotthuss C J T 1806 Sur la décomposition de l'eau et des coprs qu'elle contient en dissolution à l'aide de l'électricité galvanique *Ann. Chim.* **48** 54–74

Vuilleumier R and Borgis D 1999 Transport and spectroscopy of the hydrated proton: a molecular dynamics study *J. Chem. Phys.* **111** 4251–66

Vuilleumier R and Borgis D 2006 Molecular dynamics of an excess proton in water using a non-additive valence bond force yield *J. Mol. Struct.* **436** 555–65

Wang N, Butler J P and Ingber D E 1993 Mechanotransduction across the cell surface and through the cytoskeleton *Science* **260** 1124–7

Warach S and Baron J C 2004 Neuroimaging *Stroke* **35** 351–3

Wassall S R 1996 Pulsed field-gradient-spin echo NMR studies of water diffusion in a phospholipid model membrane *Biophys. J.* **71** 2724–32

Whittam R 1961 Active cation transport as a pace-maker of respiration *Nature* **191** 603–4

Wiggins P M 1990 Role of water in some biological processes *Microbiol. Rev.* **54** 432–49

Williams R J P 1970 The biochemistry of sodium, potassium, magnesium and calcium *Chem. Soc. Q. Rev.* **24** 331–65

Wojcieszyn J W, Schlegel R A, Wu E S and Jacobson K A 1981 Diffusion of injected macromolecules within the cytoplasm of living cells *Proc. Natl Acad. Sci. USA* **78** 4407–10

Xu X and Yeung E S 1998 Long-range electrostatic trapping of single-protein molecules at liquid-solid interface *Science* **281** 1650–3

Yablonskiy D A, Ackerman J J H and Raichle M E 2000 Coupling between changes in human brain temperature and oxidative metabolism during prolonged visual stimulation *Proc. Natl Acad. Sci.* **97** 7603–8

Yablonskiy D A, Bretthorst G L and Ackerman J J H 2003 Statistical model for diffusion attenuated MR signal *Magn. Reson. Med.* **50** 664–9

Yoshizaki K, Seo Y, Nishikawa H and Morimoto T 1982 Application of pulsed-gradient ^{31}P NMR on frog muscle to measure the diffusion rates of phosphorus compounds in cells *Biophys. J.* **38** 209–11

Zhong J, Petroff O A C, Pleban L A, Gore J C and Prichard J W 1997 Reversible, reproducible reduction of brain water apparent diffusion coefficient by cortical electroshocks *Magn. Reson. Med.* **37** 1–6

Zhong J, Petroff O A C, Prichard J W and Gore J C 1993 Changes in water diffusion and relaxation properties of rat cerebrum during status epilepticus *Magn. Reson. Med.* **30** 241–6